Urban Air Quality in Asian Mega Cities: Particulate Modeling
Model Description and Preliminary Results
- A Case Study on the Greater Seoul Area

Submitted by
Sarath K. Guttikunda

Table of Contents:

List of Tables:

List of Figures:

Figure #A7: Comparison of time series of model predicted daily average concentrations to measurements, μg PM_{10}/m^3 – Under normal meteorological conditions.

Figure #A8: Comparison of time series of model predicted daily average concentrations to measurements, μg PM_{10}/m^3 – Under horizontal wind speeds uniformly capped and scaled at 4.0 m/sec.

Figure #A9: Comparison of time series of model predicted daily average concentrations to measurements, μg PM_{10}/m^3 – Under normal meteorological conditions and with 50% cut down in emissions from unpaved road section.

1. Introduction

Over the past few decades a rapid industrialization has been observed in many of the Asian megacities, which has led to the poor or deteriorating air quality in the cities. Within cities of developing countries, rapid urbanization lead to increase in population numbers, population density, Industrial sectors, number of vehicles and hence a variety of emission sources. In view of this rapid increase in the sources of emissions, and the lack of effective strategies to control these emissions, air pollution problems affecting cities in developing countries, like those in Asia, are of particular concern. Energy consumption levels and the associated trace gas emissions for most of the Asian megacities will increase atleast two folds by 2020 (Foell, W., et al, 1995). As a result, air quality issues have become a serious environmental problem at both the regional and urban scale for many developing countries in Asia.

Increasing attention from investigators all around the world towards environmental and human hygiene resulted in conducting many epidemiological studies. A series of epidemiological studies conducted in the megacities of Asia, Europe and USA, revealed a particular concern to the relationship between the health effects and concentrations of various trace species (GEMS/AIR, 1996). The same studies also led to the statistical association between health effects and Particulate matter (PM) concentrations, usually total suspended particles (TSP) and PM_{10}. In the past, monitoring and air quality assessment studies conducted for Asian megacities has portrayed a serious concern for growing concentrations of many trace gas species like SO_2, NO_x and Ozone. World Bank reports on Urban Air Quality Management Strategy in Asia (Shah, J. J., et al, 1997) presents an outline for major steps involved in the air quality assessment studies for Asia. Also presented are the trends in primary pollutant levels for four major megacities of Asia, *viz.*, Greater Mumbai, India, Jakarta, Indonesia, Manila, Philippines and Katmandu, Nepal and possible emission abatement strategies. More on the increasing pollution level in these cities is dealt in the coming sections.

As part of the IIASA's Regional Air Pollution INformation and Simulation for Asia (RAINS-Asia) phase-II, one element of this project is focused on contributing to the development of an integrated model to assess the concentration and deposition patterns of particulate matter (TSP, PM_{10}, $PM_{2.5}$). Moreover, this work also focuses on the development of source-receptor relationships, in order to identify the potential threat associated with various emission sources to a region or a selected location. With most of the population concentrated in and around the developing areas of urban cities, the present work in confined to the development of an Urban-scale PM model. The city of Greater Seoul, South Korea will be the central focus of this work. Results include development of annual and seasonal concentration profiles for urban and suburban areas, source-receptor relationships, comparison of the model runs with measurements obtained from Korean EPA at daily, monthly and annual level. Also included are the results from uncertainty analysis of the model parameters, viz., dry deposition velocity and precipitation scavenging rates of the PM_{10}, meteorological conditions and uncertainty in the emission inventories. In view of the limitations attached to the model predictions from the development of emission factors to the use of meteorological data, this work

should be considered as only a preliminary attempt to understand the deposition and concentration profiles of particulate matter at an urban scale.

Structure of this report is as follows: Chapter-2 gives a brief description of the nature of particulate matter, their composition, air quality guidelines and past/present trends of PM for some Asian cities. ATMOS/URBAT model parameterization, meteorological fields used, emission and transport scheme in the model are discussed in Chapter-3. Also discussed is the air quality situation in Seoul area, on going work towards the assessment of health and visibility studies in Seoul and some neighboring cities in Korea. Chapter-4 focuses on energy use and PM emission fields utilized in this work, followed by a brief discussion on possible methods to improve the existing data set. In this section, two different scenarios of emissions are discussed. Chapter-5 presents model results for the simulation domain at daily and annual basis and the possible source-receptor relationships from each of the emission sources to specific locations of the domain. Figures presented in this section are the simulated annual 2-D concentration field and a time series plot of daily average concentrations for a location in the middle of the city. A brief description on PM_{10} measurements obtained from Korea EPA department, limitations associated with the measurement are discussed in Chapter-6. Site specific description, whether residential/industrial and possible influence of natural and anthropogenic sources at various measurement sites is also discussed in this section. Chapter-7 and Chapter-8 explores the uncertainties involved in the model parameters, emission estimates and variations in meteorological conditions. Results obtained from sensitivity runs conducted under each of the uncertainties are presented here, followed by conclusions in Chapter-9.

2. Particulate Matter

“Particulate Matter” is a generic term for a broad class of chemically and physically diverse substances that exists as discrete particles. Clouds of particles have names, which segregate their characteristics by size and color, like smoke, fog, haze, mist and smog. Particulate matter size ranges from 10^{-3} μm to a few microns. The chemical and physical properties of these particles vary greatly with time, region, meteorology and source category, thus complicating the assessment of health and welfare effects. A more detailed study on health effects of particulates in developing countries is presented in Panyacosit, L., 1999. Particulate matter is broadly classified into primary and secondary sources. Primary particles have both natural and man made (anthropogenic) origins. Man made sources for primary particulates are fuel combustion, road transport, industrial processes, domestic heating, etc. Among the natural sources, we have wind blown dust, sea spray, volcanoes and forest fires. Secondary particulate matter has chemical transformation of gas species to particles in the atmosphere, as their origin. Main chemical reactions include oxidation of sulfur dioxide to sulfate, oxidation of NO_x to nitrate, reduction of ammonia to ammonium salts and oxidation of hydrocarbons. A detailed literature review on sources of primary and secondary particulates presented elsewhere (Koch, M., 1998, Paranova, I., 1998 and Wilson, W.E., et al, 1997). Important removal processes associated with the particulates are deposition, coagulation due to impaction and electrostatic forces, and nucleation of submicron particles. In the process of long-range

transport, atmospheric behavior is determined by the aerodynamic size of the particles. Particles between 0.1 to 1 μm have longer residence times compared to the particles greater than 1 μm, subsequently getting transported over thousands of kilometers (Van Houdt, 1990). A rather long residence time leads to stable concentrations while the short residence time causes considerable variations, which effects the concentration profiles and the dose response analysis. Air quality standards for PM and many other trace gas species are different for different time periods. The WHO 1987 Air Quality Guidelines (AQG) for TSP are 100 $\mu g/m^3$ for annual mean concentrations and 150-230 $\mu g/m^3$ for a 24-hr mean concentration. For PM_{10}, we have 60-90 $\mu g/m^3$ for a 24-hr mean concentration.

2.1 PM Levels in Asian megaCities

Many regions of Asian megacities experience PM concentrations exceeding WHO AQG, which propels the need to develop a more stringent air quality management system to bring these pollutant levels under a safer limit. Increasing levels of TSP, PM_{10} and $PM_{2.5}$ are reported for many cities in the developing world. In the urban and industrial areas of the Greater Mumbai, TSP levels ranging from 180 $\mu g/m^3$ to 270 $\mu g/m^3$ is reported (Shah, J. J., et al., 1997). In Jakarta, concentrations in most of the polluted areas are 5-6 times the national air quality standard, with TSP levels exceeding 300 $\mu g/m^3$ (Shah, J. J., et al., 1997). Ambient TSP levels in Metro Manila are reported to vary from 115 to 256 $\mu g/m^3$ on an annual average basis, with 24-hr mean values ranging from 79 to 549 $\mu g/m^3$ at the sampling stations for the year of 1991/92. For Kathmandu, Nepal, a major tourism place is also under the threat of increasing TSP levels ranging from 321 to 474 $\mu g/m^3$ on a 24-hr average basis and 200 to 1,572 $\mu g/m^3$ on a 8-hr average (Shah, J. J., et al., 1997). It is assumed that the high concentrations of TSP are the result of heavy traffic in these commercial areas. Also reported are high PM_{10} concentration levels averaging 137 and 157 $\mu g/m^3$ on a 24-hr and 8-hr average basis respectively. Chow, J. C., et al, 1998, in their report for urban air quality management in China, reported 24-hr maximum TSP levels ranging from 210 to 2574 $\mu g/m^3$ for many Asian urban and suburban areas (Source: GEMS-1989 report). A more comprehensive report on the increasing PM concentration levels and the associated health effects is presented in Panyacosit. L., 1999.

3. Modeling System

3.1 Model description – ATMOS/URBAT

Particulate matter deposition and concentration fields for TSP, PM_{10}, $PM_{2.5}$ are calculated using the ATMOS model. This model is a modified version of the Branching Atmospheric Trajectory (BAT) model developed by the U.S. National Oceanic and Atmospheric Administration (NOAA) (Heffter, J. L., 1983). The ATMOS model is a three dimensional multi-layered lagrangian model was used to calculate sulfur deposition and sulfate concentration fields for Asia as part of IIASA RAINS-Asia phase-I project. A more detailed information of the ATMOS model formulation can be obtained from Arndt, R., 1997, Arndt, R., et al, 1998. URBAT, a modified version of ATMOS for urban

scale, is presented in Calori, G., et al, 1999. Figure #1 presents the schematics of the modeling system, inputs required and the associated pre- and post-processors. Each of the input fields mentioned in the figure is discussed in detail in this Chapter. Vis5D, a public domain visualization software, is utilized in the view the end results. TRAMP is converter developed to create transfer matrices or Source-Receptor relationships from the model predicted source specific concentration fields.

Figure #1: Modeling system schematic diagram

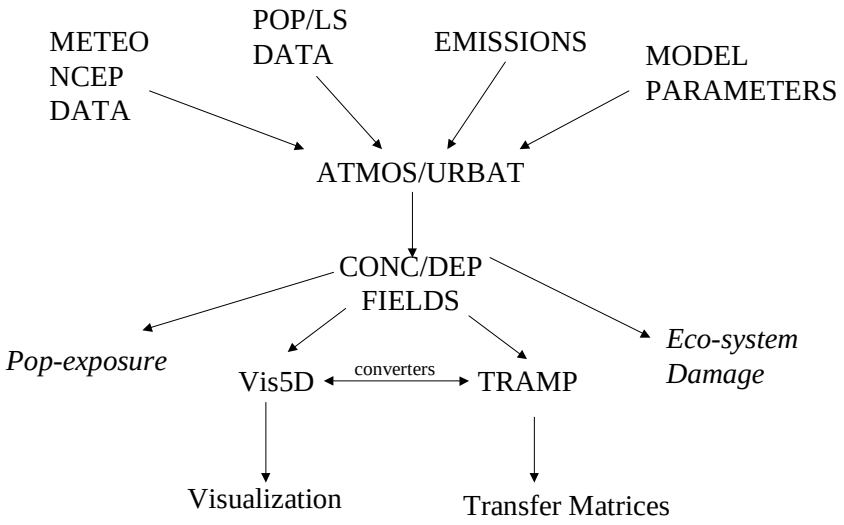

Model simulations are conducted at a resolution of 5 minutes. For modeling purposes, all the regional sources are considered as surface based sources, located at the center of 5' x 5'grid cell and released into the mixing layer during the day time and the surface layer during the night time. All the large point sources are released into the mixing layer at all times. Each puff, released every three hours, is assigned a mass proportional to the source strength, and is assumed to mix uniformly in the vertical throughout the assigned layer, and to diffuse with a guassian distribution in the horizontal. Individual puffs are followed throughout their transport and deposition lifetimes, until its mass falls below a cut-off value, or until it is transported beyond the modeling domain, whichever happens first (Arndt, R., et al, 1998). Model calculations are carried out for the target year of 1995. The model's ability to develop the source receptor relationships is utilized in the development of transfer matrices. These transfer matrices will be used in the development of an integrated RAINS module for PM. Model parameters and other inputs used are discussed in detail in the following sections.

3.1 Study domain - The Greater Seoul

Asian megacities are increasing in number as well as in size. With the increasing urbanization and growing population density, more people are susceptible to increasing levels of pollutants. Some of the Asian megacities of interest are Mumbai (India), Manila

(Philippines), Jakarta (Indonesia), Bangkok (Thailand), Shanghai (China) and Seoul (South Korea). This study concentrates on the growing pollution levels of the city of Greater Seoul, South Korea, located in the northwestern part of the country on the Han River, 37 miles from the Yellow Sea. The input domain extends from 37° to 38° in latitude and 126°25′ to 127°30′ in longitude, covering cities of Seoul, Inchon and rest of Kyonggi district. The simulation domain extends from 36°40′ to 38°20′ in latitude and 126°05′ to 127°50′ in longitude. Figure #2 presents the input domain and the districts under consideration. Also presented in Figure #2, is the land sea mask for the domain, the gray shade corresponds to land and the population distribution of the domain, with most of the population concentrated around city of Seoul. Population distribution at a 5' x 5' resolution is obtained from NCGIA, 1995. Estimated population for 1990 for the city of Seoul is 11 million and it is projected to exceed the 13 million mark by the year 2000 (Ezcurra, E., et al, 1996). The size of Seoul (605 km^2) is only 0.6 % of the South Korea, but has 25% of the population, 32% of the vehicles and provides more than 40% of total national production. Estimated population growth for the decade of 1980-1990 is 2.9% with a per capita GDP for 1991 of US $6,277 and an annual GNP growth rate of 8% (Ezcurra, E., et al, 1996). Estimated per capita income level in South Korea for 1997 is over US $10,000 (National Geography, Oct'98). With a bludgeoning economy like this, before the Asian crisis in the late 1998, and a strong industrial revolution in the cities of South Korea, led to some severe air pollution problems.

Figure #2: Population distribution for the Greater Seoul area

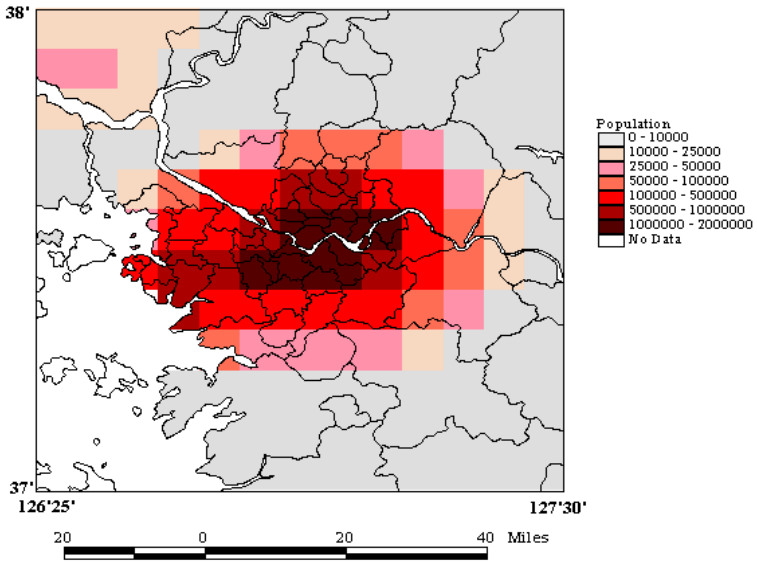

Monitoring studies conducted in the past for areas in and around Seoul presents trends in increasing health and environmental impacts, for both indoor and outdoor conditions. Visibility studies conducted by Baik, N., et al, 1996, reveal a growing impact of PM emissions on visibility in Seoul area for varying PM chemical composition and size. Baik et al observed a 80% and 55% light extinction during the smoggy and clear periods, strongly driven by diurnal variation in temperature and thus the mixing heights. Kim, et al., 1998, Baek, et al., 1997, Hashimoto, et al., 1994, Chung, et al., 1999, presents the

quantitative contribution, chemical and temporal analysis of aerosols for many areas of South Korea. Baek, et al., 1997, also presents quantitative distribution of the TSP in urban, suburban and industrial areas of Korea. Mean average TSP concentrations measured by many of these researchers for the cities of Korea ranged between 83 to 172 $\mu gm/m^3$ for urban and rural areas. The contribution to secondary particulate matter varies over a wide range with many trace gas species like sulfates, nitrates, ammonium salts and trace elements like As, Fe, K, Mg, Mn, Ni, Pb, Se, Ti, V, Zn, etc (Chung, et al., 1999 and Hashimoto, et al., 1994). Most of the species originate from fuel combustion in vehicles, small and large industries and power plants. Above mentioned studies also monitored the chemical composition of PM, a detailed review on the chemical composition from various monitoring studies is presented in Koch, et al, 1998.

South Korea's climate is characterized by a cold, relatively dry winter and a hot, humid summer. The coldest average monthly temperatures in winter drop below freezing except along the southern coast. The average January temperature in Seoul is about -5°C, while the corresponding average at Pusan, on the southeast coast, is 2°C. By contrast, summer temperatures are relatively uniform across the country, the average monthly temperature for August (the warmest month) being about 25°C. Annual precipitation ranges from about 900 to 1,500 mm on the mainland. A wide range of variation in annual temperature is observed in Seoul's climate and heavy precipitation during the summer months. With half of the simulation domain covered by industrial sites and widely spread urban area, urban island heating raises inland temperatures by a few degrees (Park, H., 1986 and Lee, H., 1993).

3.2 Meteorology

Meteorological data for this project is obtained from the NCEP/NCAR Reanalysis project (NCEP, 1998). A more detailed description of the available datasets can be obtained from *http://www.cdc.noaa.gov/cdc/data.nmc.reanalysis.html*. For this study, horizontal wind fields and accumulated precipitation fields for the year of 1995, for every 6-hr at 2.5 x 2.5 degree resolution are obtained from this reference. Other parameters utilized include surface pressure, surface temperature, horizontal surface wind fields, and surface heat sensitivity flux. Later parameters are used in the calculation of mixing heights. Figure #4 presents a time series of accumulated precipitation field for the simulation domain. It can be noticed that the precipitation is high during the summer season, more than 60% of the total precipitation received in that grid cell, compared to ~15% during spring and fall. During summer, Seoul area receives precipitation as high as 4.5 mm/hr (averaged over a 6hr-time period), with an average precipitation rate of 0.2 mm/hr during the late summer and early fall. A little over 16% of the time, the simulation domain receives a precipitation of 0.1 mm/hr, threshold rate of precipitation and over 16% of the time precipitation of 0.01-0.1 mm/hr.

From the 3-D wind fields obtained from NCEP-reanalysis, back trajectories are developed to and from Seoul area (figures not presented in this report). These studies indicate possibilities of long transport of dust from desert areas in China and from volcanic sources in Japan. On going modeling studies on the long-range transport of dust

at University of Iowa, USA and Kyushi University, Japan will provide more information on the percentage contribution from these periodic dust storms to local PM concentrations in Seoul Region. Also, during the summer, sea sprays contribute to a significant amount towards the local PM concentrations, especially around the coastal regions. Measurement campaigns conducted in and around Cheju Island, south of South Korea presents a strong signal from sea sprays and similar studies have been conducted near the Inchon port area. Using a detailed meteorological data set (NCEP), it is possible to explore the impacts of log-range transport of episodic dust storms, volcanic emissions and sea sprays. This section of analysis is yet to be explored.

Mixing height or the critical inversion height designates the top of the model's boundary layer and the bottom of its upper layer. Mixing heights are calculated according to Carson, J. D., 1983 and Venkatram, A., 1980. 3-D Wind fields, precipitation rates and mixing heights used are interpolated to a 5' x 5' resolution using bilinear interpolation scheme.

Figure #3: A time series of accumulated precipitation rates in mm/hr and frequency of occurrence at 127°E and 37.5°N

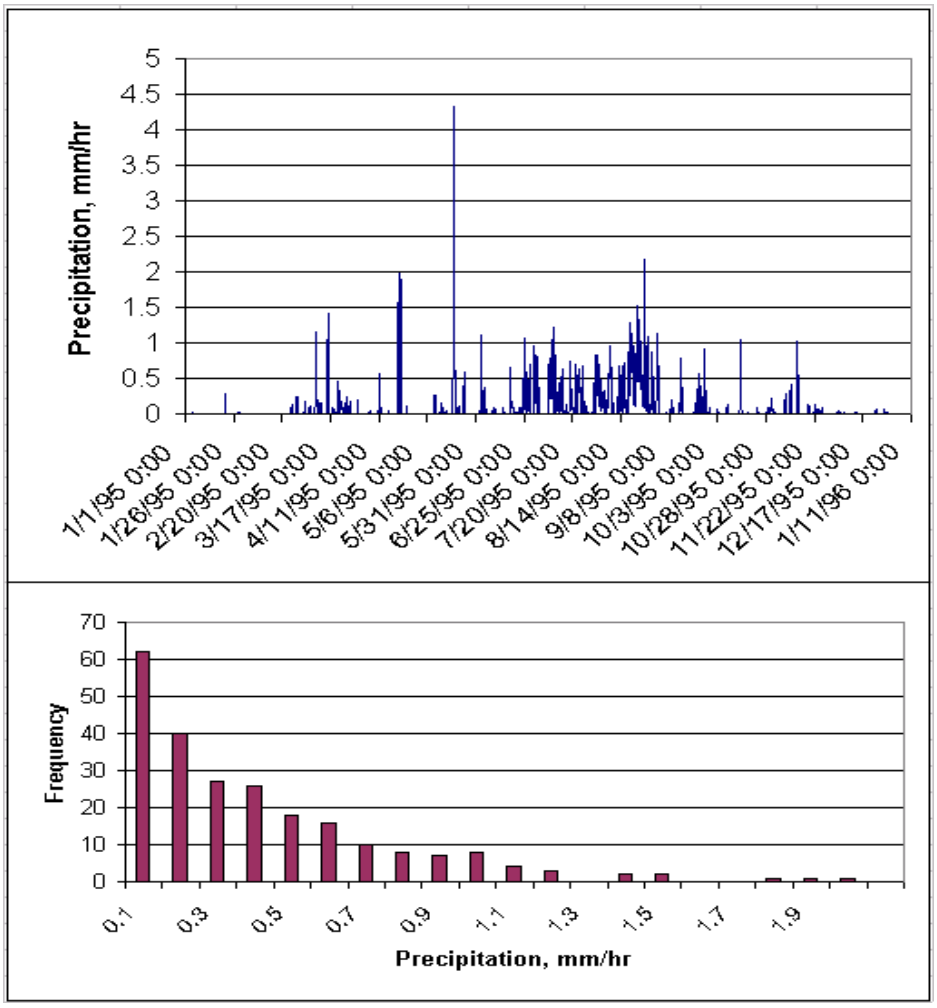

3.3 Model parameters

Table #1 lists all the important model parameters utilized. Removal processes considered in this study are only dry and wet deposition processes. For the time being, no coagulation or nucleation process is considered. The removal of particulate matter and gases at the air surface interface is described generically in meteorological transport models by the terms of "dry deposition" or "dry deposition velocity". A net removal rate at the surface from dry deposition is calculated using the following equation.

$$R_d = \frac{V_d}{z}$$

where, R_d is the removal rate, V_d is the dry deposition velocity from Table #1 in m/sec, and z is the height of the surface layer in m, depending on the day/night transitions and the stability zones. Deposition velocities have been measured in field conditions by the artificial deposition collection surfaces, using selected surfaces within a vegetative canopy, and also by calculating deposition velocities from airborne concentrations in both urban and rural environments. The deposition velocities for gases range over four orders of magnitude, and the deposition rates for particles range over three orders of magnitude (Sehmel, G. A., 1980). A summary of the dry deposition velocity estimates is presented in Table #2. Clearly, the results of these studies cover a wide range and some authors have attempted to explain some of the range by invoking meteorological factors.

Precipitation scavenging of the particulate matter is also considered and it is scavenging rates are calculated according to the following equations.

$$R_w = S_p * p$$

where, R_w is the precipitation scavenging rate, S_p is the precipitation scavenging coefficient in cm^{-1} from Table#1, and p in precipitation in m/hr. The wet scavenging coefficients used in the previous regional and global models for PM/aerosol studies are presented in Table#3.

Background concentrations are important for an urban scale study, especially for places like Seoul, which has sources from not only the intra-city activities, but also from sea sprays, volcanic sources and dust storms mentioned before. Model runs are conducted without any background concentrations. It will be included in the future modifications of the model. Re-suspension of the particles dry deposited forms a substantial amount of the source term. A 10% re-suspension term in incorporated in the model for the time steps and grids, where the accumulated precipitation doesn't exceed the threshold value of 0.1 mm/hr. Model is run for both with and without re-suspension to see the differences incurred due to this physical process. An increase of 2-10% in the concentration fields is obtained from without and with re-suspension runs. To account for the vast difference in the physical and chemical properties of PM_{10} and $PM_{2.5}$ fractions, the model is run for two different bins, *viz.*, PM_{10}-$PM_{2.5}$ and $PM_{2.5}$ and the results are added together at the end for sensitivity and comparison studies.

Table #1: Parameter used in ATMOS long-range transport model for particulate model

Parameter	Explanation, unit	Value
V_{ds}, PM_{10}	Dry deposition velocity for PM_{10} over sea surface, cm/sec	0.7
V_{dl}, PM_{10}	Dry deposition velocity for PM_{10} over land, cm/sec	0.6-4.0
V_d, $PM_{2.5}$	Dry deposition velocity for $PM_{2.5}$ over sea and land surfaces, cm/sec	0.1
H, surface	Surface layer height, m	300
H, top	Upper layer height, m	6000
S_j	Wet deposition rate of PM_{10} and $PM_{2.5}$ over land and sea, cm^{-1}	2.5
Resus	Resuspension for periods with precipitation less than threshold value of 0.1 mm/hr	10 %
	Background concentrations, $\mu g/m^3$	None
Dt	Transport time step, hr	1
	Emission puff release time step	3
	Concentration and deposition field output time step	Variable

Table #2: Literature review on dry deposition velocities of PM used in previous global and regional models

Source	Size fraction	Methodology, Conditions, etc	Deposition Velocity, cm/sec
Sehmel, G. A., 1980	1-10 μm	Literature review and modeling. Reported for Natural aerosol deposition on land surface.	0.8
Williams, R. M., 1982	2.5 μm	Modeled for deposition over Natural water surfaces. Wind velocity between 2-20 m/sec.	0.1-1.2
Williams, R. M., 1982	10 μm	-do-	0.7-1.2
Slinn, S.A. and W. G. N. Slinn, 1980	2.5 and 10 μm	Modeled for deposition of particles over Natural waters by impaction. Wind velocity between 1-15 m/sec	0.3-1.2
Peters, K. and R. Eiden, 1992	2.5 μm	Measurements and Modeling for deposition of particles over Spruce forest. Wind velocity between 0.5 to 5 m/sec	0.06-1.3
Peters, K. and R. Eiden, 1992	10 μm	-do-	1.2-200
Allen A.G., R. M. Harrison and K. W. Nicholson, 1991	0.1 – 2.0 μm	Measurements under rainy, sunny and cloudy conditions. Wind velocity = 4.0 cm/sec (mean).	0.1 +/- 0.18
Walton, J. J., M. C. MacCracken and S. J. Ghan, 1988	>1.0 μm	Parameters from Global scale lagrangian trace species model	1.0

Walton, J. J., M. C. MacCracken and S. J. Ghan, 1988	< 1.0 μm	-do-	0.2
Liousse, C., J.E. Penner, C. Chung, J. J. Walton, H. Eddleman and H. Cachier, 1996	0.1 – 2.0 μm	Parameters from global model for carbonaceous aerosols.	0.1
Chen, S. J., C. C. Lin and S. C. Chu, 1998	1.8 – 3.2 μm	Measurements and modeling of particle deposition flux for urban areas	0.02
Chen, S. J., C. C. Lin and S. C. Chu, 1998	5.6 – 10 μm	-do-	0.82 for urban 0.62 for rural
Cooke, W. F. and J. J. N. Wilson, 1996	1.0 μm	Parameters from global black carbon model	0.1
Cadle, S. H., J. M. Dasch and P. A. Mulawa, 1985	Different trace species	Measurements and calculations of deposition velocities to snow	0.1 – 2.1
Noll, K. E and K. Y. P. Fang, 1989	Variable size	Dry deposition model for PM, dependent on wind speed and PM size	
Van Jaarsveld, J. A., 1995	Variable size	Dry deposition velocity for PM chart	

Table #3: Literature review on precipitation scavenging rates of PM used in previous global and regional models

Source	**Size Fraction**	**Methodology, Conditions, etc**	**Precipitation Scavenging rate, cm^{-1}**
Penner, J.E., H. Eddleman and T. Novakov, 1993	Fine particles (BC)	Parameters from global black carbon model	0.7 for convective 2.5 for Stratoform
Cooke, W. F. and J. J. N. Wilson, 1996	-do-	Parameters from global black carbon model	2.5
Walton, J. J., M. C. MacCracken and S. J. Ghan, 1988	Supermicron	Parameters from Global scale lagrangian trace species model	3.0 for convective 8.0 for Stratoform 8.0 for snow
Walton, J. J., M. C. MacCracken and S. J. Ghan, 1988	Submicron	-do-	0.3 for convective 1.0 for Stratoform 1.0 for snow

4. Energy use and Emissions

Not many studies have been conducted on developing the emissions inventories for particulate matter at urban and regional scales. On going research at IIASA, proposes to develop a module as part of RAINS software, to generate PM emission inventories for Europe and Asia. Shah, J. J., et al, 1997 (a, b, c &d) has presented a comprehensive report on the air quality of the four megacities of Asia, *viz*. Mumbai, Jakarta, Manila and Katmandu. Reports suggest that there has been a gradual change in the energy use and emissions over the last couple of decades in these cities. A similar change in the energy demand cycle has been observed in the city of Greater Seoul, South Korea. 1995 as the target year, a preliminary emission inventory estimates for TSP, PM_{10} and $PM_{2.5}$, for the Seoul area was developed at IIASA (Lee, S., 1998). In this study only primary PM sources are considered. Most of the emission factors used for the emission estimates are obtained from U. S EPA, 1998 and Shah, J. J., 1997 a-d. A comprehensive report on the emission factors from studies conducted in Europe, US and Asia can be obtained from Koch, M., 1998 and Paunova, I., 1998. From here on, the term PM_{10} implies the PM faction in the size range of 2.5 μm to 10 μm and $PM_{2.5}$ is the particulate matter faction below 2.5 μm.

Sources of particulate matter vary widely in size, composition and type of release (surface in case of automobiles, etc or elevated in case of power stacks). Industrial and motor vehicle emissions are believed to be major sources of PM emissions in Korea (Baek, S., 1997). Some of the major primary PM sources considered in this report are listed below.

- Fugitive dust from construction, storage piles, and vehicle traffic on paved and unpaved roads. The last sections form the major portion of the emissions in the form of fugitive dust.
- Vehicle exhaust from cars (passenger and taxi), trucks (heavy and light), motorcycles, medium buses (also considered is the type of fuel used, gasoline and diesel), and heavy buses (city, intercity, rented, express and others).
- Fuel combustion in the household: vegetative burning from stoves, coal burning, trash, and agricultural waste burning.
- Ducted exhaust from industrial facilities such as power plants, cement plants, steel mills, incinerators, chemical plants, petroleum refining, and glass manufacturing.
- Large point and small point sources from power plants, domestic heating and industrial processes.

Some of the processes and sources not included in this modeling study are as follows:

- Fugitive dust from wind erosion, long-range transport of dust of the dust storms, agricultural activities (like use of fertilizers) and animal husbandry.
- Particulate matter from chemical reactions, such as sulfates from SO_2, nitrates from NO_x, ammonium salts from ammonia emissions and from hydrocarbon reactions.

Emission estimates from Lee, S., 1998 for the Greater Seoul area, including Inchon city and Kyonggi district are summarized here. Table#4 presents the quantitative and Figure#4 the spatial distribution of the emissions from various sources mentioned above for PM_{10} and $PM_{2.5}$ factions respectively. A total of 1033 ktons of TSP, 383 ktons of PM10 and 137 ktons of PM2.5 as PM emissions are estimated from Seoul area. As mentioned earlier, emissions from paved and unpaved roads form a major source of particulate matter in Seoul region. Approximately 70% for PM_{10}-$PM_{2.5}$ and approximately 50% for $PM_{2.5}$ faction coming from unpaved roads. Unpaved roads here are probably roads still under construction and under regular repair conditions.

Vehicular emissions form a significant part of $PM_{2.5}$ emissions, which is of major concern to health studies in the populated areas. Of the six major emission sources mentioned, most of the fugitive dust off the paved and unpaved roads is concentrated in the most populated region of Seoul. From the gridded population distribution and the spatial distribution of emissions from vehicles and fugitive dust off paved/unpaved roads, a strong correlation between the two density functions can be observed. It can be inferred that the use of more vehicles, and added features of AC and heating facilities are more prevalent in the urban areas than the rural, contributing to more of PM emissions from these sources. This results in increased population exposure, premature mortality and morbidity rates, and many respiratory related diseases.

Most of the industrial groups from Seoul and Inchon cities are concentrated near the coastal areas, owing to PM emissions from this sector spreading to the west and southwest of the city. Figure #4 also presents the large points sources, with most of them centered in the Inchon district. Contribution from Inchon to the emissions base is mainly from the industrial sector. The same is true for the emissions from small point sources (power plants and industrial sectors). Point sources from heating follows the vehicular emission pattern with a direct dependency on the population density distribution. High industrial emissions from Inchon district is due to the presence of the major shipping port. PM emissions from shipping activities are not included in this study, which might of significant importance in a trading center like Inchon. There are no emissions estimated for $PM_{2.5}$ faction under Industrial processes. There are a lot uncertainties involved in the emission estimates and this study should be considered as a preliminary step towards the development of a module makes use of various source categories in assessing the impact of PM emissions on environment and human hygiene.

Table #5 presents the percentage contributions from various sectors to TSP, PM_{10} and $PM_{2.5}$ factions under two different scenarios – A1 and B1. Scenario A1 presents the percent of emissions presented in Lee, 1998. From EPA reference sites, (US-EPA, 1998), estimating PM emissions, scenario B1 assumes that most of the unpaved roads are converted to paved, cutting down fugitive dust of unpaved roads by atleast 50%. ATMOS model is run for these two scenario’s and results are presented in Chapter-8.

Table #4: PM emissions in the Greater Seoul area for 1995, tons of PM

		Paved roads	Unpaved roads	Point sources	LPS	Vehicles	Ind_processes	Total (Ktons)
	TSP	184385	746460	2446	6416	59831	32976	1033
A	PM10	35340	268726	1678	3439	59024	15215	383
	PM2.5	8451	70914	1090	1983	54179	0	137
	PM10-PM2.5	26889	197812	588	1455	4845	15215	247

Figure #4: Gridded PM Emissions in the Greater Seoul area for 1995, tons of PM

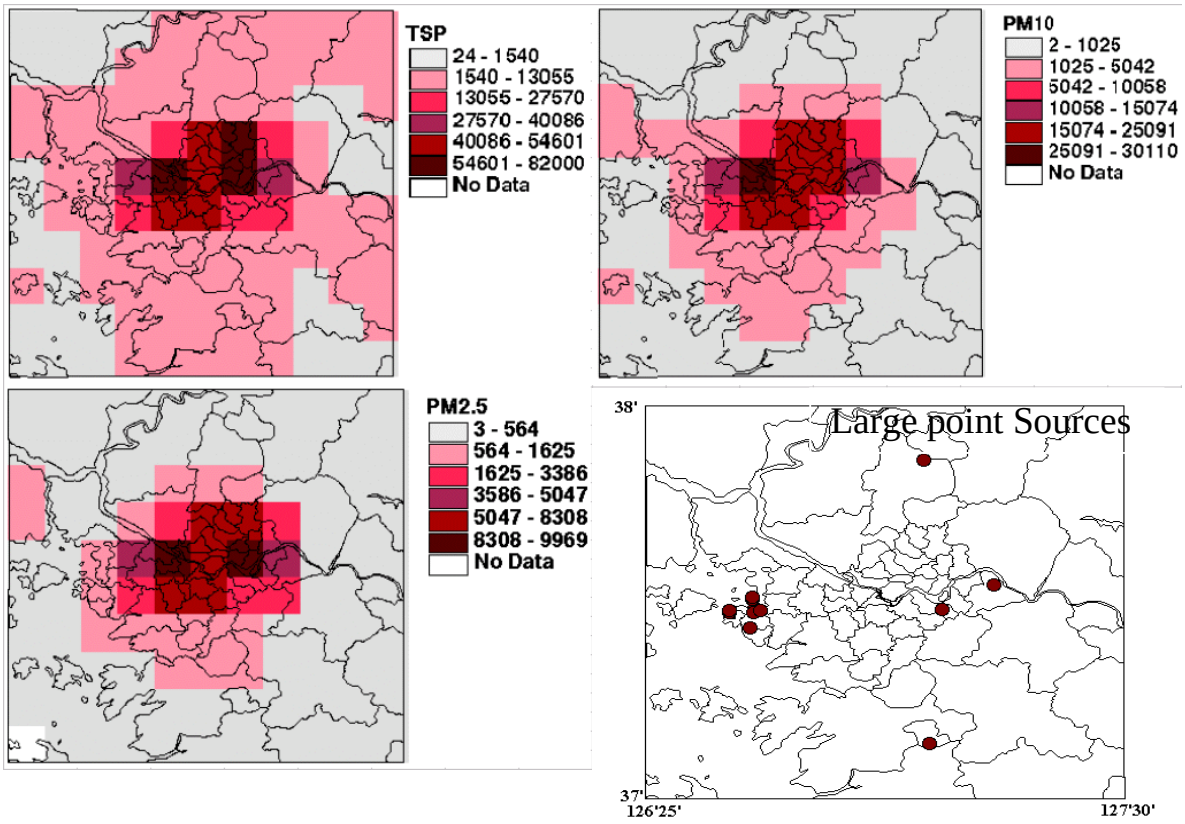

Table #5: Sectoral percentage contribution to PM emissions in the Greater Seoul area for 1995

	%%	Paved roads	Unpaved roads	Point sources	LPS	Vehicles	Ind_processes
	TSP	18	72	0	1	6	3
A1	PM10	9	70	0	1	15	4
	PM2.5	6	52	1	1	40	0
	PM10-PM2.5	11	80	0	1	2	6

	%%	Paved roads	Unpaved roads	Point sources	LPS	Vehicles	Ind_processes
	TSP	28	57	0	1	9	5
B1	PM10	14	54	1	1	24	6
	PM2.5	8	35	1	2	54	0
	PM10-PM2.5	18	67	0	1	3	10

5. Results

5.1 Annual PM levels

Annual deposition and concentration fields are calculated using the ATMOS/URBAT model for TSP, PM_{10} and $PM_{2.5}$. To account for the differences in the deposition patterns for particles < 2.5 μm and > 2.5 μm, the model is run separately for the PM_{10}-$PM_{2.5}$ and $PM_{2.5}$. Figure#5 presents the model predicted annual averaged concentration in $\mu g/m^3$ for PM_{10} and $PM_{2.5}$ respectively. Model results presented used an average dry deposition velocity of 2 cm/sec over the urban areas, 0.7 cm/sec for the water bodies (for PM_{10} faction) and 0.1 cm/sec (for $PM_{2.5}$ faction) and a precipitation scavenging coefficient of 2.5 cm^{-1} for both the factions. These results include emissions from all the sectors, *viz.* power, transport, industrial and fugitive dust off the paved and unpaved roads under scenario A1. Dry deposition velocity utilized for this particular run is the average of the range of values obtained from literature survey, and shouldn't be considered as final parameter value. More of the results from sensitivity runs of dry deposition velocity are presented in the coming sections. Concentration profiles follow the emission pattern, with peak concentrations occurring over the densely populated areas. Annual average concentrations exceeding WHO-AQG of 90 $\mu g/m^3$ are predicted for most of the populated regions of simulation domain.

Figure#5: Model predicted annual average PM_{10} and $PM_{2.5}$ concentrations in the Greater Seoul area for 1995, μg PM_{10}/m^3

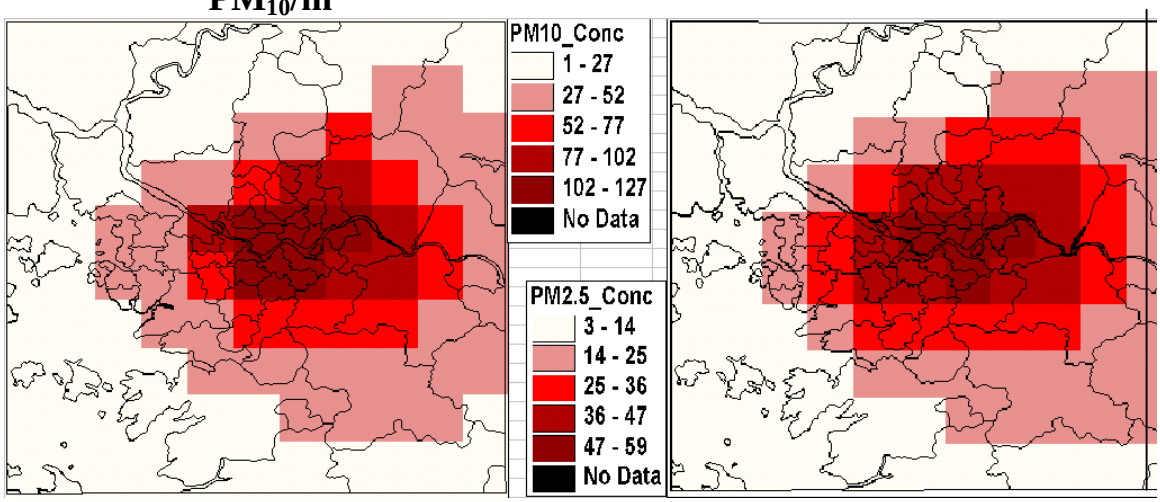

5.2 Daily average concentration profiles

For the parameters listed in Table#2, daily average concentrations of PM_{10} and $PM_{2.5}$ are also estimated. Figure #6 presents a time series plot for PM_{10} and $PM_{2.5}$ of the daily average concentrations at 127°E and 37.5°N. Spatial and temporal variation in concentration profiles is observed at different measurement sites, sending strong signals

towards meteorological features of the study domain. Also presented are monthly moving averages for the simulation period. Monthly average PM_{10} and $PM_{2.5}$ concentrations ranged from 60-200 $\mu g/m^3$ and 40-120 $\mu g/m^3$ for this location. Overall, in the vicinity of the city, daily average concentrations ranged from 50-500 $\mu g/m^3$. Particularly, high daily average concentrations in the months of summer and fall are attributed to higher precipitation rates and strong winds. For the same coordinates, Figure #7 presents correlation between predicted PM_{10} and $PM_{2.5}$ concentrations. Similar kind of correlation is also observed during monitoring studies conducted in some of the Asian cities. (Lam, et al., 1999 and Shah, J., et al., 1997)

Figure #6: Time series of model predicted PM_{10} and $PM_{2.5}$ daily average concentrations at 127°E and 37.5°N, μg PM_{10}/m^3

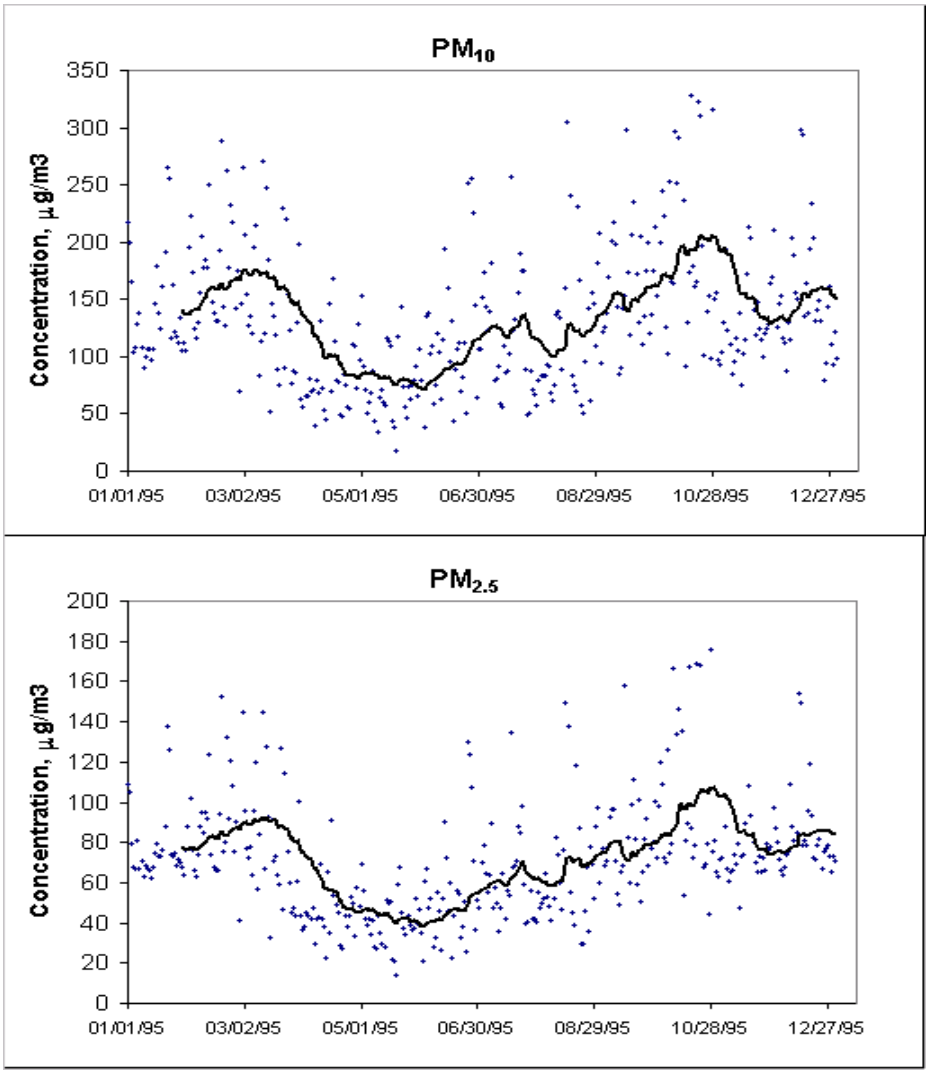

Figure #7: Correlation between model predicted daily average PM_{10} and $PM_{2.5}$ Concentrations at 127°E and 37.5°N, μg PM_{10}/m^3

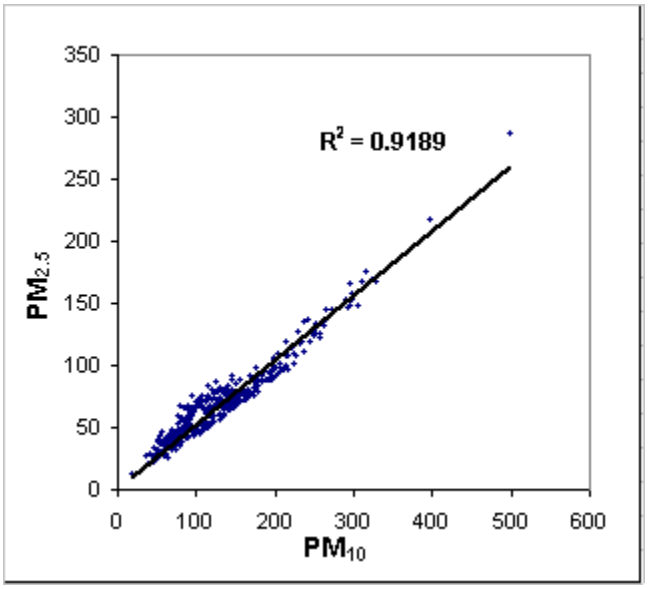

5.3 Population exposure

It's been well established that the PM is one of the major precursors linked to adverse health effects like premature mortality and morbidity related health end points (Ostro, 1996). People are constantly being exposed to high concentrations of PM both indoor and outdoor in most of the developing countries. Studies conducted for industrial and residential areas have developed some dose response relationships for health effects associated with PM to the number of hours/days of exposure to concentrations exceeding the AQG. Table #9 presents the number of days that the concentrations exceeded the daily PM_{10} AQG of 90 μg/m^3 and higher concentration at a given location. However, from the concentration profiles, it's the population in and around the Seoul area that is constantly exposed to the growing PM levels.

5.4 Source-Receptor relationships

The understanding of source-receptor relationship has become a central issue in the air quality management. The source-receptor relationship is the impact of specific sources and/or source types upon a receptor concentration. ATMOS model allows the construction of source-receptor relationships on a grid to grid basis or region to grid basis or source to grid basis – determining the role of meteorology and physical/chemical effects linking source emission to receptor concentration. This principle was utilized in the development of the RAINS-Asia and RAINS-Europe emission/deposition models for Sulfur, NOx and Ozone protocols, to understand the policy implications on emission control strategies at both regional and national levels. The same methodology can be applied here at an urban scale to understand the contribution of various emission sources

to the ambient PM levels and thus giving way to the development of more rational emission control policy.

Table #6: Percentage Sectoral Contribution to Annual Average PM_{10} and $PM_{2.5}$ Concentration at Selected locations in the Greater Seoul for 1995

PM_{10}	Paved	Unpaved	Vehicles	Ind_process	Small PS	LPS
Yeonhee	8	55	22	5	1	10
Gyeyang	8	57	21	5	1	8
Sinsol	7	74	17	1	0	0
Hogye	9	63	21	4	1	1
$PM_{2.5}$						
Yeonhee	5	43	39	0	1	12
Gyeyang	5	45	39	0	1	10
Sinsol	5	58	36	0	0	1
Hogye	7	49	42	0	1	2

The source – receptor relationships from six emission sources for the Greater Seoul region (extending from 36°40′ to 38°20′ in latitude and 126°05′ to 127°50′ in longitude) will be provided in the digital format, which can be applied to the future emission database developments. The relationships provided are grid-to-grid matrices covering all the six emission sources. Under small point sources section, heating, power plant and small industrial sources are combined together due to the limitations in the model pollutant transport scheme. Model is run with a threshold puff size of 10 tons/year. However, for the construction of grid-to-grid matrices, all the grids with emissions less than the threshold value of 10 tons/year are simulated for 100 tons/year to construct a proper source-receptor relationship from each grid to the study domain. As an example, Table #6, presents percentage contribution from six different PM sources to the four stations in Greater Seoul area. Vehicular emissions are more important in case of $PM_{2.5}$ faction and so is the fugitive dust from paved and unpaved roads. There is no contribution from Industrial processes to PM2.5 emissions. Fugitive dust off the roads due to higher silt content and particle size, it is more concentrated in the PM_{10}-$PM_{2.5}$ faction.

6. Measurements

Air quality monitoring forms an important aspect of Air Quality Assessment. Monitoring results can be used to conduct epidemiological studies, to investigate source identification and apportionment to study the long-range transport phenomena, and to establish more cost-effective plans to control air pollution. Monitoring of particulate matter needs to be focused on different aspects of behavior of particles in air. Composition and concentrations of particulates will differ in space, time and season due to emission type, chemical reactions and meteorology. This leads to a lot of uncertainties in the evaluation of the model results and also in the development of Dose-Response curves. For this particular study, measurements for PM_{10} are obtained from Korean EPA, for 18 different stations in and around the city of the Greater Seoul, whose locations are listed under Table#7 and graphically represented in Figure#8. Of these 18 stations, 11 are residential

areas and the rest industrial. Of these, 10 stations belong to city of Seoul, 6 to city of Inchon and the rest two to Kyonggi province. Measurement sites are located at a height of 10 m above the ground level.

Figure#8: Network of monitoring stations selected for model comparison

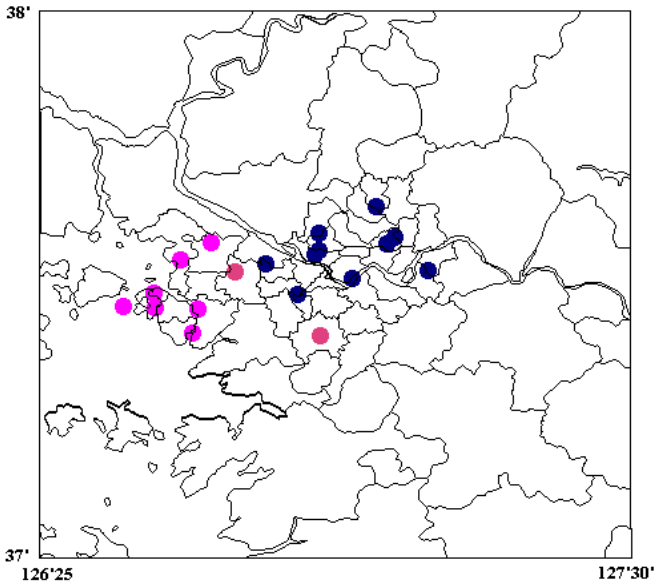

Figure#A1 presents the daily average concentrations measured at these stations. Spatial and temporal variation in the concentrations can be observed throughout the study domain. However, the location of the sites is also taken into consideration during the comparison to the model results. For the stations, very near to the Inchon seaport are not included in the comparison study, since the emissions from shipping activity and sea sprays is not taken into consideration, which happens to contribute a substantial fraction of secondary PM sources, especially in the nitrates and sulfates at these locations. For example, Mansuck, a highly industrialized area next to the port attached to it, contributes significantly to the PM emissions under industrial sector. A sample comparison of the model results and measurements taken for this station are presented if Figure#A2 (Figure with a dot on right hand-top corner). From the Figure#A2, it is evident that the model is under-predicting for the most part of January and July, which suggests the lack of data from sources other than industries. Also, Kwanghwamum is a measurement site located in the middle of the downtown, and center of the palace, which makes it a remote station. Similarly, Kuwol, a province to the south of the Seoul, is edged by a major industrial complex to it's south, which makes it vulnerable to the summer sea breeze, drifting more of the emissions to this highly residential area. Keeping these uncertainties in mind, model results are compared with measurements at different levels, discussed in detail in Chapter-8. All the measurement, comparison and model sensitivity analysis figures are presented under Appendix #A.

Table #7: Network of monitoring stations and PM_{10} Measurements, μg PM_{10}/m^3

Station	Long	Lat	Annual Average, μg/m^3
Kwanghwamun (DT)	126.93	37.56	84.4
Myonmok (R)	127.06	37.58	87.7
Sinsol (R/SF)	127.05	37.57	94.0
Ssangmun (M)	127.03	37.64	81.7
Pulgwang (R)	126.93	37.59	64.1
Mapo (R)	126.95	37.54	76.1
Hwagok (R)	126.83	37.53	72.4
Kuro (I)	126.89	37.48	60.7
Panpo (R)	126.99	37.51	81.4
Pangi (R)	127.13	37.52	57.6
Sinheung (I)	126.63	37.45	100.0
Mansuck (I/P)	126.625	37.48	67.1
Yeonhee (R)	126.675	37.54	76.8
Gyeyang (R)	126.73	37.57	72.7
Kuwol (R/I)	126.71	37.45	93.6
Sungui (I)	126.57	37.46	73.6
Nae (I)	126.78	37.52	69.6
Hogye (R)	126.93	37.40	77.6

R =Residential, DT =Downtown, I =Industrial, SF =Small Factory, M =Mountains

Table #7 also presents the annual average values for all the 18 stations. Not all stations have measurements for 365 days. Average concentrations for these stations are calculated on the basis of available data only. Annual average value ranged from 57 – 94 μg/m^3 with daily averages ranging from 4 – 845 μg/m^3. Model predicted daily average concentrations for January and July are compared with the measured values for some of the stations listed in Table#7.

7. Uncertainties

As mentioned in the previous sections, there are uncertainties at every stage of modeling studies. Some of the uncertainties considered in this study are

- Uncertainty in the model parameters
  - Dry deposition velocity of PM_{10} fraction
  - Wet scavenging rates for PM_{10} and $PM_{2.5}$ factions.
- Uncertainty in the emission estimates, this includes the lack of relevant information on the emission factors for Korea, which lead to the use of the US. EPA and URBAIR reports for the emissions estimate.

- Uncertainty in the meteorological processes, like not considering the process of urban island heating during the calculation of mixing heights and the thermal characteristics of urban fabric and the urban geometry.
- Uncertainties due to the omission of natural sources of particulate matter like sea sprays, volcanoes and soil erosion off the agricultural regions.
- Uncertainty due to the omission of secondary particulate chemistry and the physical processes like coagulation and nucleation in the model.
- Uncertainty in the measurements, which is always questionable during the comparison and model sensitivity studies.

7.1 Dry deposition and Precipitation scavenging rates

Dry deposition velocities and the Wet scavenging rates are varied for the range of values specified in Table #2. Six stations for the month of January and the month of July are selected to compare the model results and to study the sensitivity of the model to parameter variation. Dry deposition for $PM_{2.5}$ fraction was maintained constant at value 0.1 cm/sec irrespective of land/sea cover and for the PM_{10}-$PM_{2.5}$ fraction at 0.7 cm/sec over the water bodies, details of which are presented in Table#3. Over the land, the dry deposition velocity for PM_{10}-$PM_{2.5}$ fraction is varied between 1.0 and 4.0 cm/sec, taking into consideration all the measurement studies and the dry deposition velocity models used for previous gas-to-particulate and aerosol modeling studies.

7.2 Emission estimates

As can be seen from the emission distribution, both sectoral and spatial, one of the major uncertainty lies in the estimates of PM emissions from fugitive dust of the unpaved roads. From the comparison plots presented in Appendix-A, especially for the stations, with the urban/populated area, where the vehicular and unpaved road emissions contribute the most, one can say that the apportionment of the uncertainty in these emission estimates is quite appropriate. A model run is conducted under this scenario, with a 50% cut down of the fugitive dust off unpaved roads, variations in model predictions of which are presented in Appendix-A.

Many of the natural sources of particulate matter, like volcanoes, sea sprays, which form a major source of emissions for regions like Seoul close to the water bodies and countries dominated with huge volcanoes, like Japan. This is considered as one of the major uncertainties, especially due to the fact that these sources are mainly responsible for the background concentrations of PM because of the higher residence times, their release mechanisms, and also the long-range transport.

Inchon, being one of the major industrial and shipping areas of East Asia, with the major port attached to the study domain, it is necessary to consider the emissions from daily shipping trade activities. Apart from the ship emissions, one more major sector that has been omitted during the emission estimates is from the agricultural runoffs from the rural areas surrounding the city of Seoul, Inchon and Kwonggi.

7.3 Wind speed in the lowest layer

For the model simulations, meteorology from NCEP reanalysis is utilized. The net wind speed for many of the grid cells ranged from 0.1 – 15 m/sec and the values are interpolated to the model resolution of 5'x5' using the bilinear interpolation scheme. From many of the dry deposition velocity measurement campaigns and air quality monitoring studies, the average wind speed in the urban areas ranged from 1 – 4 m/sec, see Table#3. Also wind tunnel experiments with model structures, blockades, etc., to simulate a city environment provide information on meteorological behavior in and urban boundary layer. The process of urban island heating, which leads to the temperature anomalies in the urban and rural areas (Park, 1986) plays an important role during the mixing height calculations (ICUC'96). Presently mixing height calculations are conducted using only surface wind speeds, surface temperature, 3-D temperature fields, surface pressure and surface heat sensitivity from NCEP reanalysis. PM measurement campaigns conducted by Chung et al, 1999, for two of the cities, south of Seoul, presents an average wind speed of 1.2 m/sec for fall and winter seasons, 1.5 m/sec for summer season and a 1.9 m/sec for spring season. Because of this urban heating phenomena and blockades of different shapes and sizes around the city, urban climatology is different from the normal meteorological conditions available. To simulate urban environment, under a simplistic approach, model is run for horizontal wind speeds capped of 4.0 m/sec and uniformly scaled to 4.0 m/sec. Comparison of model results thus obtained from one such run, for the two months of January and July are presented in Figure#A5.

7.4 Secondary particulate chemistry

Secondary particulate matter, which originate from the sources other than the natural dust sources, form a major part of PM, especially in the fine particle bin. Major sources of secondary particulate matter are

- Oxidation of SO_2 from combustion processes to sulfates
- Oxidation of NO_x species to nitrates
- Reduction of NH_3 to ammonium salts of sulfur and nitrogen
- Oxidation of hydrocarbon species, mainly from vehicles

Many regional and global models have the secondary particulate chemistry in their model parameterization. EMEP model (Tarrason, et al., 1998), developed to study the policy implications in the European union has developed a secondary particulate module, which addresses the issues of contribution of sulfates and nitrates to the net particulate concentration in the atmosphere. Unfortunately, secondary particulate chemistry is not included in this study. Chemistry presented in Ackermann et al., 1995 and Binkowski, et al., 1995 will be utilized in the future modifications of the model. This is one of the potential reasons for the large deviations in the comparison of model results to the measurements.

8. Discussion

This section focuses on the discussion of the sensitivity of the model to the avalibale databases and the model parameters. Model runs are conducted for the target year of 1995. Model runs conducted in two different bins for particles < 2.5 μm and particles > 2.5 μm are clubbed together for the final comparison to the measurements from Korean EPA. The model results compared to the measurements obtained from Korean EPA are presented in Appendix A. Since, the ultimate goal of this project is to develop source receptor relationships at both source and regional level, a major focus is lead on the evaluation of model on a annual basis, rather than on a small temporal basis. However, initial comparison are conducted on a daily average basis, to understand the model's capability to replicate the meteorological and emission patterns, which is demonstrated fairly in the model results. Also, due to the availability of the measurement data for PM_{10} alone, model is evaluated for only this bin.

Figure #A1, presents the measurements obtained from the Korean EPA department as mentioned in the earlier sections. Figure #A2, presents the time series of model predictions and measurements for six different stations. Mansuck, Yeonhee and Gyeyang, to the west of Seoul, Kwanghwamum, Sinsol, in the Seoul downtown, Kuwol, to the south of Seoul and Hogye, between Inchon industrial area and Seoul, for the months of January and July. Unfortunately, not all stations have measurements for all days of the year. For this set of runs, dry deposition velocity is varied from 1.0 cm/sec to 4.0 cm/sec over land, 0.7 cm/sec over water bodies for particles > $PM_{2.5}$ μm and 0.1 cm/sec for particles < $PM_{2.5}$ μm. For all the model runs, precipitation scavenging rate is maintained at 2.5 cm^{-1}. From the comparisons presented in Figure #A2 (with dots on left hand top corner), it is evident the under-predictions of the model both in January and July that for Mansuck, closer to Inchon port is very much affected by the shipping activities. Similarly for Kwanghwamum and Kuwol, both residential but highly affected by the downtown activities and industrial activities surrounding the region respectively have over predictions. For the same reasons, these stations have been eliminated from the comparison studies, at both daily and annual level, even though the annual average concentrations are at par to many other monitoring episodes conducted in and around the city of Seoul. Nevertheless, one interesting feature of this comparison is that the model is able to capture the synoptic features of the measurements. Some of these features are discussed in detail in the coming sections. It in no means indicate that the other 15 stations are better off compared to the ones eliminated.

Figure#A2 also presents the time series of PM_{10} daily average concentrations compared to the measurements for stations Yeonhee, Gyeyang, Sinsol and Hogye for the months of January and July. Dry deposition velocity for particles > 2.5 μm over land is varied from 1.0 – 4.0 cm/sec in this analysis. Stations selected form a basis for different backgrounds. Yeonhee and Gyeyang, both residential areas with a annual average PM_{10} concentration of over 72 $\mu g/m^3$, are closer to the water bodies and gives an indication of the impact of change in the dry deposition velocity from land to sea. Model is able to capture peaks for this episode, even though the model is still under-predicting for both the stations, for

reasons discussed before. For July, Sinsol, a monitoring station close to small factories and categorized as residential area, Yeonhee, Hogye, residential areas between the urban Seoul and Inchon district are selected to compare the model predictions. As is the case in January, model is able to fairly capture most of the features from measurements. One of the observations from these figures is that the model is not as sensitive to the dry deposition velocity of the particles > 2.5 μm over land, as expected. However, the variation to the concentrations at peak events is of significant importance, which needs to be explored in detail.

Table#8: Variation of the model predicted annual average concentrations (μg PM_{10}/m^3) to the dry deposition velocity and precipitation scavenging rates

Station	Predictions	Measure-ments		Station	Predictions	Measure-ments
Myonmok	105-149	87.7		Pangi	108-155	57.6
Sinsol	107-150	94.0		Sinheung	21-31	100.0
Ssangmun	86-123	81.7		Yeonhee	28-42	76.8
Pulgwang	74-106	64.1		Gyeyang	33-50	72.7
Mapo	82-116	76.1		Kuwol	31-46	93.6
Hwagok	59-84	72.4		Sungui	15-22	73.6
Kuro	70-99	60.7		Nae	45-65	69.6
Panpo	97-136	81.4		Hogye	60-87	77.6

Figure #A3 presents the sensitivity of model predictions to dry deposition velocity of particles > 2.5 μm over land and precipitation scavenging coefficient. In this figure annual average concentrations obtained under 12 different sets of model parameters are compared to the measurements. The two lines correspond to 50% and 200% compliance limits. Similar to what observed in Figure#A2 for daily average concentration comparisons, the sensitivity to dry deposition velocity is very small. Table#8 above presents the variation in model predicted values for the 12 different runs. One an average model is able to capture the measured average concentrations. But, one should bear in mind that the model doesn't include all the possible emission fields as discussed in the previous section and the results can be better.

From the measurements, predicted concentration profiles and the back trajectories of the wind fields, there is room for improvement in the deposition and transport schemes implemented. It is observed from daily average time series that there is a seasonal component to the deposition and the transport of particles is a possible suggestion. Even though, back trajectories suggest a possible inflow of dust from desert storms and volcanic eruptions as sources to Seoul's PM emissions, one should bare in mind that even these are episodic and highly dependent of meteorological conditions. Korea experiences an inflow of dust during the dust storm periods from Gobi desert mostly during summer (Phadnis, et al, 1999). During a dust storm period, dust mass loading can be as high as 1000 $\mu g/m^3$. To illustrate the impact of the seasonal component associated with the

deposition patterns, model runs are conducted with and without seasonal component of the dry deposition velocity. For the months of April to September, a dry deposition velocity of 2.0 cm/sec and 0.8 cm/sec for the rest of the months is assumed for particles > 2.5 μm over land. Rest of the model parameters maintained constant. For no seasonal component case, deposition velocity is maintained at 2.0 cm/sec for particles > 2.5 μm over land. Figure #A4 presents the comparison of model predicted annual average concentrations for the 15 stations under these two scenarios. Also, presented are the model results under the scenario of running all the emissions under 10 μm as one bin and with no variation in the dry deposition velocity with land/sea mask. The red line corresponds to the 1-1 correspondence. From the figure, the variation in the model runs, with and without seasonal component is very small, approximately 9%. For the same reason, no seasonal component is assumed for the results presented hereafter. However, the model runs with all the emissions under one bin, *viz.*, PM_{10}, and with no difference in the dry deposition velocity of the particles for land/sea masking, varied to a great extent from the ones with no-seasonal component, approximately 16-34%. This run has been conducted just to see the sensitivity of the model to the land/sea mask. But, fact remains the same, that the particles behave differently for size ranges < 2.5 μm and > 2.5 μm and also with the land/sea mask.

As discussed under previous section, urban heat islands play an important role in the transport and deposition of gases and particles within the city. Also, due to the blockades within the city, wind velocities tend to decrease within the city limits. Taking this into considerations, ATMOS model inputs are modified to reduce the horizontal wind speed in the lowest layer uniformly throughout the study domain. All the wind speeds above 4.0 m/sec are uniformly scaled down to 4.0 m/sec and Figure #A5 presents the time series plot of comparison of model predicted values to measurements for the months of January and July for the stations in Figure#A2. Dry deposition velocities are maintained constant for this set of runs at 2.0 cm/sec over land and 0.7 cm/sec over sea for particles > 2.5 μm, and 0.1 cm/sec for particles < 2.5 μm. Dotted line corresponds to measured daily average concentrations and the other to model predicted. The results doesn't look that different from the ones presented in Figure#A2. Under this scenario, more of the daily variations in concentrations are captured compared to the previous comparisons. In the month of July, for Sinsol, model still over predicts, but the extent of over prediction has come down at least 2 folds, which suggests that the model is more sensitive to the meteorological conditions than to the dry/wet scavenging rates. Under this scenario, simulates urban environment in a simplified manner, model is able to capture more of the synoptic features than under full fledged meteorological conditions.

Emission estimates are of major concern during model evaluation. As mentioned before, due to the lack of availability of the emission factors for Korea, most of them are obtained from URBAIR and EPA reports (Lee, S., 1998). As discussed before, with most of the natural sources missing, and also due to some uncertainties in statistical database for other sources, emissions estimated from this study are expected to low on an overall basis and high in some sectors like fugitive dust off the unpaved road sections. Also, spatial distribution is of utmost importance during modeling study. Emissions from vehicular and fugitive dust sources, tend to concentrate more in the densely populated

areas than the city outskirts, whereas all the industrial sources concentrate near the coastal areas, with small factories closer to residential areas. Fugitive dust from unpaved roads is mostly concentrated in the middle of the simulation domain, mostly urban, which contributes to a substantial amount to concentrations exceeding the AQG guidelines. See Table#6 for source contributions for locations within the city limits. A set of sensitivity runs with fugitive dust off the unpaved roads cut down by 50% from all the grid cells and results thus obtained are compared to both normal meteorological fields from NCEP as well as for horizontal wind fields uniformly capped and scaled at 4.0 m/sec. Parameters used for these runs are maintained constant to those used in Figure#A5. Figure #A6 presents the comparison of model predicted annual average concentrations to the measurements. For this set of runs, all sources are processed under one bin of particles < 10 μm. Total emission inventory for the simulation domain come down from 383 ktons to 249 ktons of PM, percentage contribution from different sources under this scenario (B1) are presented in Table#5. From Figure#A6, model is under-predicting, as expected, due to lack of full set of input data. However, correlation between model predictions and measurements improved by a significant amount from previous runs.

For the four stations in Figure#A5, time series of daily average concentrations are extracted and compared to measured values. Under this set of analysis, three different scenarios are considered. Figure #A7 presents comparison of model predicted averages for runs under normal meteorological conditions and emission scenario A1. Figure#A8 presents the same for runs conducted with uniformly capped and scaled horizontal fields at 4 m/sec and emission scenario A1. Figure#A9 presents results from runs conducted under normal meteorological conditions and emission scenario B1. The two black lines correspond to 50% and 200% compliance limits. Also presented in Table#9 are the no of days the concentrations exceed the AQG guideline of 90 $\mu g/m^3$ and higher concentrations for both measured and predicted set of values for the four stations.

Table #9: No of days measured and model predicted daily average concentrations exceed a certain limit

(a) Under normal meteorological conditions (Emissions-A1)

Exceedance	Yeonhee		Gyeyang		Sinsol		Hogye	
$\mu g/m^3$	M	P	M	P	M	P	M	P
90	104	33	80	45	144	221	77	114
100	82	31	64	39	112	193	56	89
120	42	26	29	33	63	152	35	67
150	17	13	13	18	20	106	12	40

M = Measurement, P = Model Prediction

(b) Under uniformly scaled meteorological conditions (Emissions-A1)

Exceedance	Yeonhee		Gyeyang		Sinsol		Hogye	
$\mu g/m^3$	M	P	M	P	M	P	M	P
90	104	40	80	48	144	342	77	163
100	82	34	64	42	112	330	56	142

120	42	27	29	36	63	288	35	115
150	17	18	13	23	20	194	12	75

M = Measurement, P = Model Prediction

(c) Under normal meteorological conditions (Emissions-B1)

Exceedance	**Yeonhee**		**Gyeyang**		**Sinsol**		**Hogye**	
$\mu g/m^3$	M	P	M	P	M	P	M	P
90	104	27	80	34	144	203	77	99
100	82	21	64	24	112	174	56	70
120	42	11	29	16	63	124	35	34
150	17	6	13	8	20	55	12	8

M = Measurement, P = Model Prediction

From the figures, for the areas closer to the sea, viz., Yeonhee and Gyeyang, which belong to Inchon city, we see that model under predicts for most part of the year. One of reasons for this could be the negligence of contributions from natural sources, shipping activity and secondary sources. For the other two stations, most of the predictions, fall between the compliance lines, suggesting a lesser probability of missing emissions sources, but a uncertainty within the estimation of emission factors and emissions themselves still exist. Table#10 presents the correlation coefficients obtained for each location under the three scenarios discussed above. Correlation coefficient increased gradually from scenario in A7 to A9. Mainly, for the regions west of Seoul, significant increase in the coefficient strengthens the fact that fugitive dust off the unpaved road section was one of the key players in determining PM levels outside the Seoul area.

Table #10: Correlation analysis from time series comparison of daily average concentrations to measurements

Station	**No. of Meas.**	**Correlation Coefficient**			**% times between factor of 2**		
		Fig#A7	Fig#A8	Fig#A9	Fig#A7	Fig#A8	Fig#A9
Yeonhee	354	0.0006	-0.0555	-0.0454	21	35	29
Gyeyang	354	-0.1855	-0.3251	-0.4138	32	44	37
Sinsol	297	-0.0096	-0.3513	-0.3309	65	57	80
Hogye	247	-0.0383	-0.2013	-0.2703	51	58	65

From the tables above, model is able to predict the no of days, concentrations exceeded AQG guidelines and higher limits to a fair extent, even though the day of predictions is off for most of the time.

9. Conclusions

As part of the RAINS-Asia Phase-II project, ATMOS three dimensional lagrangian model is developed to study the deposition and transport properties of particulate matter at urban and regional level. Model is evaluated for the Greater Seoul Region, South Korea. Concentration and deposition profiles are compared to the measurements obtained

from the Korean EPA. Sensitivity of the model to model parameters and the input databases is studied to understand the model's ability to replicate the real conditions. At the end source-receptor relationships are developed for future use. Major conclusions following the analysis are summarized here. Model performance is against model parameters like dry deposition velocity and precipitation scavenging rates of PM. It's observed that the sensitivity of the model predictions to these parameters is less than expected. Measured annual average concentrations ranged from 57-100 $\mu g/m^3$ for model predictions for the same locations ranged from 15-155 $\mu g/m^3$. Sensitivity of the model to change in urban climatology is also conducted, by capping all the horizontal wind speeds and uniformly scaling them to a value of 4.0m/sec. Model results from various scenarios compared fairly well to the measurements obtained from Korea EPA department. Several measures are under consideration to try to capture more of the synoptic features in the model predictions like in daily and monthly averages. Use of real meteorological fields made available from NCEP Reanalysis, made it possible to conduct in-depth analysis on urban climate within the city of Seoul. Part of the proposed work to improve model behavior are- inclusions of a more detailed PM emission inventory, in-depth analysis on the urban island heating effect and it's impact on mixing height calculations, and inclusion of secondary particulate chemistry mainly sulfates and nitrates. This study being the first of it's kind, the results presented here are very preliminary.

Bibliography

Ackermann, I. J., H. Hass, M. Memmesheimer, C. Ziegenbein and A. Ebel, 1995. The parameterization of the Sulfate-Nitrate-Ammonia aerosol system in the long transport model EURAD. *Meteorology and Atmospheric Physics,* Vol. 57, pp. 101-114.

Alcamo, J. and J. Bartnicki, 1987. A framework for error analysis of a long-range transport model with emphasis on parameter uncertainty. *Atmospheric Environment,* Vol. 21, pp. 2121-2131.

Allen, A.G., R. M. Harrison and K. W. Nicholson, 1991. Dry deposition of fine aerosol to a short grass surface. *Atmospheric Environment,* Vol. 25A, pp. 2671-2676.

Arndt, R. L., 1997. The role of sulfur emissions on Asia's environmental change: Analysis on a regional and urban scale. Ph. D. Thesis, The University of Iowa, Iowa City, USA.

Arndt, R. L., G. R. Carmichael and Roorda, J. M., 1998. Seasonal source-receptor relationships in Asia. *Atmospheric Environment*, Vol. 32, pp. 1397-1406.

Baek, S., J. Choi and S. Hwang, 1997. A quantitative estimation of source contributions to the concentrations of atmospheric suspended particulate matter in urban, suburban and industrial areas of Korea. *Environmental International,* Vol. 23, pp. 205-213.

Baek, S., Y. Kim and R. Perry, 1997. Indoor air quality in homes, offices and restaurants in Korean urban areas – indoor/outdoor relationships. *Atmospheric Environment,* Vol. 31, pp. 529 544.

Baik, N., Y. P. Kim and K. C. Moon, 1996. Visibility study in Seoul, 1993. *Atmospheric Environment,* Vol. 30, pp. 2319-2328.

Binkowski, F. S. and U. Shankar, 1995. The regional particulate matter model, 1. Model description and preliminary results. *Journal of Geophysical Research*, Vol. 100, pp. 26191-26209.

Cadle, S. H., J. M. Dasch and P. A. Mulawa, 1985. Atmospheric concentrations and the deposition velocity to snow of nitric acid, sulfur dioxide and various particulate species. *Atmospheric Environment,* Vol. 19, pp. 1819-1827.

Calori, G. and G. R. Carmichael, 1999. A trajectory model for sulfur in Asian megacities: Model concepts and preliminary results. *Atmospheric Environment*, Vol. 33, pp. 3109 - 3117.

Carson, D. J., 1973. The development of a dry inversion-capped convectively unstable boundary layer. *Quarterly Journal of Royal Meteorological Society,* Vol. 99, pp. 450-467.

Chen, S. J., C. C. Lin, and S. C. Chu, 1998. Dry deposition modeling of Nitrate and Sulfate by using particle size distribution data. *Journal of Environmental Science and Health,* Vol. 33(2), pp. 307-334.

Chow, J. C. and J. G. Watson, 1998. Measurement and modeling methods for assessing environmental impacts of fugitive dust and other sources : Capacity building for urban air pollution management in China – Particulate control, Strategies in Xi'an, Shaanxi province. Report submitted to *United Nations Project # CPR/96/306/A/01-99.*

Chung, Y. S., J. H. Moon, Y. J. Chung, S. Y. Cho, and S. H. Kang, 1999. Study on air pollution monitoring in Korea using low volume air sampler by instrumental neutron activation analysis. *Journal of Radioanalytical and Nuclear Chemistry,* Vol. 240(1), pp. 79-94.

Cooke, W. F. and J. J. N. Wilson, 1996. A global black carbon aerosol model. *Journal of Geophysical Research,* Vol. 101, pp. 19395-19409.

Ezcurra, E. and M. Mazari-Hiriart, 1996. Are megacities viable? A cautionary tale from Mexico City. *Environment,* Vol. 38, pp. 6-35.

Foell, W., C. Green, M. Amann, S. Bhattacharya, G. R. Carmichael, M. Chadwick, S. Cinderby, T. Haugland, J. P. Hettleingh, L. Hordijk, J. Kuylenstierna, J. J. Shah, R. Shrestha, D. Streets and D. Zhao, 1995. Energy use, emissions, and air pollution reduction strategies in Asia. *Water, Air and Soil Pollution,* Vol. 85, pp. 2277-2282.

GEMS/AIR, 1996. Air quality Management and assessment capabilities in 20 major cities. *Environment Assessment Report – UNEP/DEIA/AR.96.2,* The Monitoring and Assessment Research Center, London.

Hashimoto, Y., Y. Sekine, H. K. Kim, Z. L. Chen and Z. M. Yang, 1994. Atmospheric fingerprints of East Asia, 1986-1991. An urgent record of aerosol analysis by the Jack network. *Atmospheric Environment,* Vol. 28, pp. 1437-1445.

ICUC'96, 1999. Special issue: International Conference on Urban Climatology 1996. *Atmospheric environment,* Vol. 33, pp. 3877-4222.

Kim, P. and C. Rho, 1986. Size distribution of atmospheric aerosols in Seoul. *Atmospheric Environment,* Vol. 20, pp. 1837-1845.

Kim, Y., J. H. Lee, N. J. Baik, J. Y. Kim, S. Shim and C. Kang, 1998. Summertime characteristics of aerosol composition at Cheju island, Korea. *Atmospheric Environment,* Vol. 32, pp. 3905-3915.

Koch, M., 1998. Airborne fine particles in the environment: Health effects, environmental studies, modeling strategies and implications for abatement strategies. Interim report under preparation. IIASA, Laxenburg, Austria.

Lam, G. C. K., D. Y. C. leung, M. Niewiadomski, S. W. Pang, A. W. F. lee and P. K. K. Louie, 1999. Street level concentrations of nitrogen dioxide and suspended particulate matter in Hong Kong. *Atmospheric Environment,* Vol. 33, pp. 1-11.

Lee, H., 1993. An application of NOAA AVHRR thermal data to the study of urban heat islands. *Atmospheric Environment,* Vol. 27B, pp. 1-13.

Lee, S., 1998. A case study of estimation of particulate matter emitted in Greater Seoul. Report submitted to IIASA, Laxenburg, Austria.

Liousse, C., J. E. Penner, C. Chung, J. J. Walton, H. Eddleman and H. Cachier, 1996. A Global three-dimensional model study of carbonaceous aerosols. *Journal of Geophysical Research*, Vol. 101, pp. 19411-19432.

NCEP, 1999. NCEP Reanalysis data obtained from NOAA, National Meteorological Center, USA.

NCGIA, 1995. Global population of the world. *NCGIA Technical report TR-95-6*. David Simonett Center for Spatial Analysis, University of California, Santa Barbara, USA.

Noll, K. E. and K. Y. P. Fang, 1989. Development of a dry deposition model for atmospheric coarse particles. *Atmospheric Environment*, Vol. 23, pp. 585-594.

Ostro, B., 1996. A methodology for estimating air pollution health effects. *Technical report WHO/EHG/96.5*. World Health Organization, Geneva.

Panyacosit, L., 1999. Particulate Matter and Health: A Focus on Developing Countries. Interim report under preparation. IIASA, Laxenburg, Austria.

Park, H., 1986. Features of the heat island in Seoul and its surrounding cities. *Atmospheric Environment,* Vol. 20, pp. 1859-1806.

Paunova, I., 1999. Towards integrated assessment of particulate matter air pollution: Contribution analysis of sources and emissions of atmospheric particles. Interim report under preparation. IIASA, Laxenburg, Austria.

Penner, J. E., H. Eddleman and T. Novakov, 1993. Towards the development of a global inventory for black carbon emissions. *Atmospheric Environment*, Vol. 27A, pp. 1277-1295.

Peters, K. and R. Eiden, 1992. Modeling the dry deposition velocity if aerosol particles to a spruce forest. *Atmospheric Environment,* Vol. 26A, pp. 2555-2564.

Peters, K. and G. Bruckner-Schatt, 1995. The dry deposition of gaseous and particulate nitrogen compounds to a spruce stand. *Water, Air and Soil Pollution,* Vol. 85, pp. 2217-2222.

Phadnis, M. J. and G. R. Carmichael, 1999. Influence of mineral aerosol on the tropospheric chemistry in East Asia. Submitted to *Journal of Atmospheric Chemistry.*

Seinfeld, J. H. and S. N. Pandis, 1998. Atmospheric Chemistry and Physics of Air Pollution – Atmospheric combustion, global cycles and lifetimes. Published by *John Wiley & Sons Inc.*

Sehmel, G.A., 1980. Particle and gas dry deposition. *Atmospheric Environment,* Vol. 14, pp. 983-1011.

Shah, J. J. and T. Nagpal, 1997. World Bank Technical Reports No. 378-381: URBAIR Urban Air Quality Management Strategy in Asia – Kathmandu Valley, Jakarta, Metro Manila and Greater Mumbai reports.

Slinn, S. A. and W. G. N. Slinn, 1980. Predictions for particle deposition on natural waters. *Atmospheric Environment,* Vol. 14, pp. 1013-1016.

Tarrasón, L and S. Tsyro., 1998. Long-range transport of fine particles, as presently estimated by the EMEP lagrangian model. EMEP-MSC-W report, July, 1998.

U. S. EPA, 1996. Air quality criteria document for particulate matter: Volume I (EPA 600/P-95/001aF); Volume II (EPA 600/P-95/001bF); Volume III (EPA 600/P-95/001cF).

U. S. EPA, 1998. Compilation of air pollutant emission factors, EPA AP-42.

Van Houdt, J. J., 1990. Mutagenic activity of airborne particulate matter in indoor and outdoor environments. *Atmospheric Environment,* Vol. 24B, pp. 207-220.

Van Jaarsveld, J. A., 1995. Modelling the long-term atmospheric behaviour of pollutants on various spatial scales. Ph. D. Thesis, Universiteit Utrecht, The Netherlands.

Venkatram A., 1980. Estimating the Monin-Obukhov lenght in the stable boundary layer for dispersion calculations. *Boundary Layer Meteorology,* Vol.19, pp. 481-485.

Walton, J. J., M. C. MacCraken and S. J. Ghan, 1988. A global scale lagrangian trace species model of transport, transformation and removal processes. *Journal of Geophysical Research,* Vol. 93, pp. 8339-8354.

Williams, R. M., 1982. A model for the dry deposition of particles to natural water surfaces. *Atmospheric Environment,* Vol. 16, pp. 1933-1938.

Wilson, R. and J. Spengler, 1996. Particles in our air : Concentrations and health effects. Published by *Harvard University Press*.

Wilson, W. E. and H. H. Suh, 1997. Fine particles and coarse particles: Concentration relationships relevant to epidemiologic studies. *Air & Waste Management Association,* Vol. 47, pp. 1238-1249

Appendix A

Figures from Model Sensitivity Analysis

Figure #A1: Time series of daily measurements taken at 18 stations in the city of Greater Seoul for 1995, μg PM_{10}/m^3

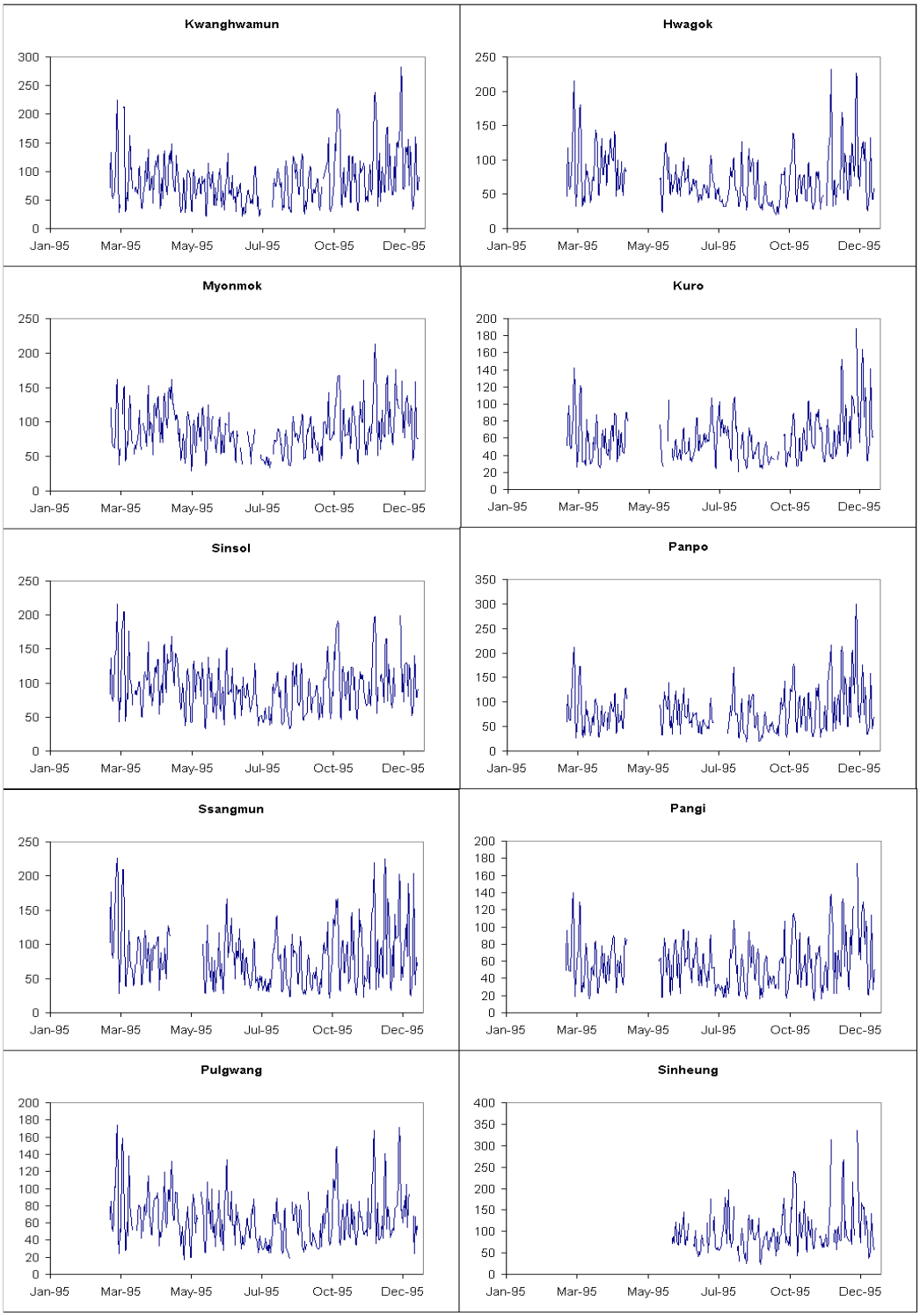

Figure #A1: Daily average measurements (contd ..)

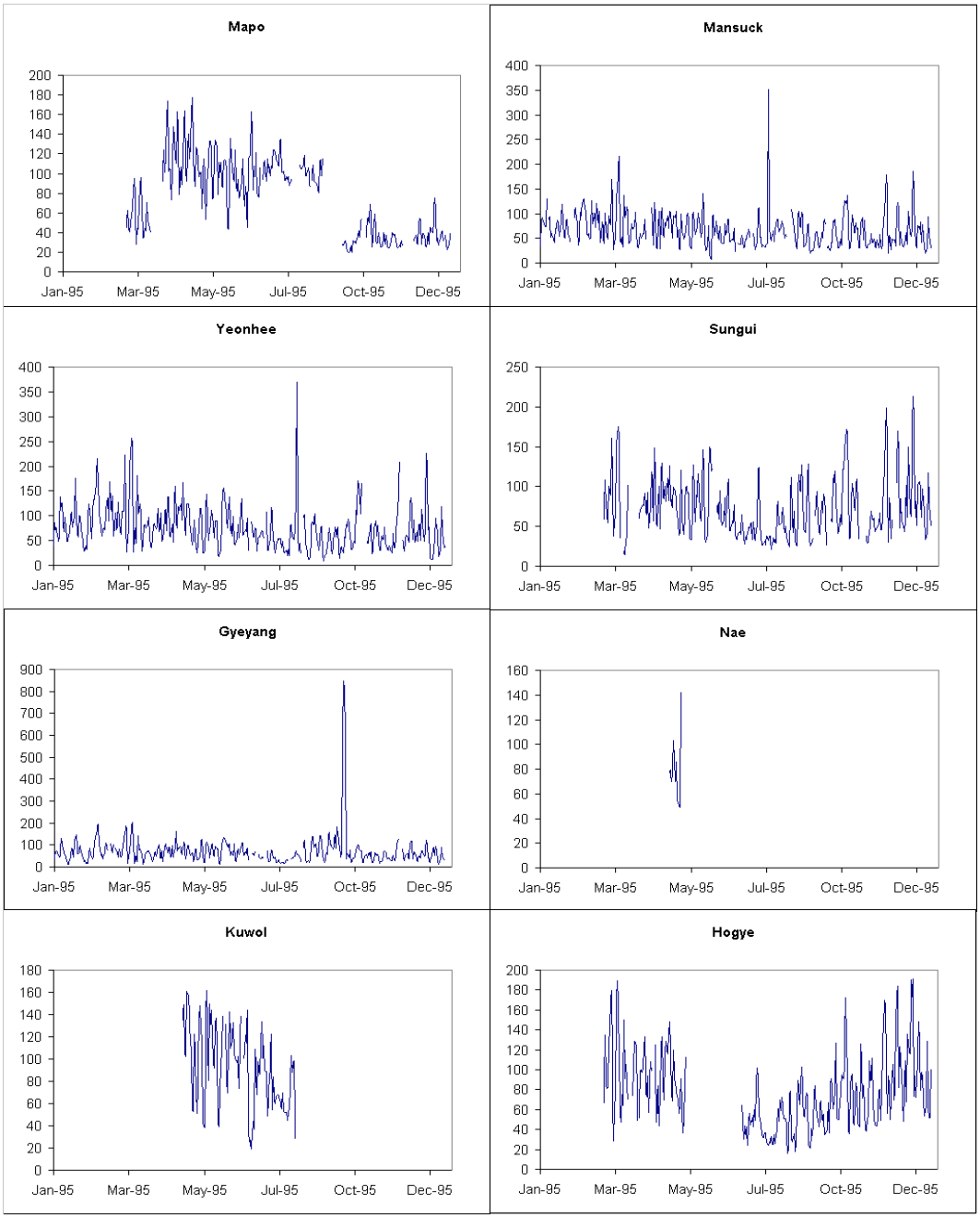

Figure #A2: Sensitivity of model predictions to dry deposition velocity over land – Comparison to daily average measurements for the months of January and July, μg PM_{10}/m^3

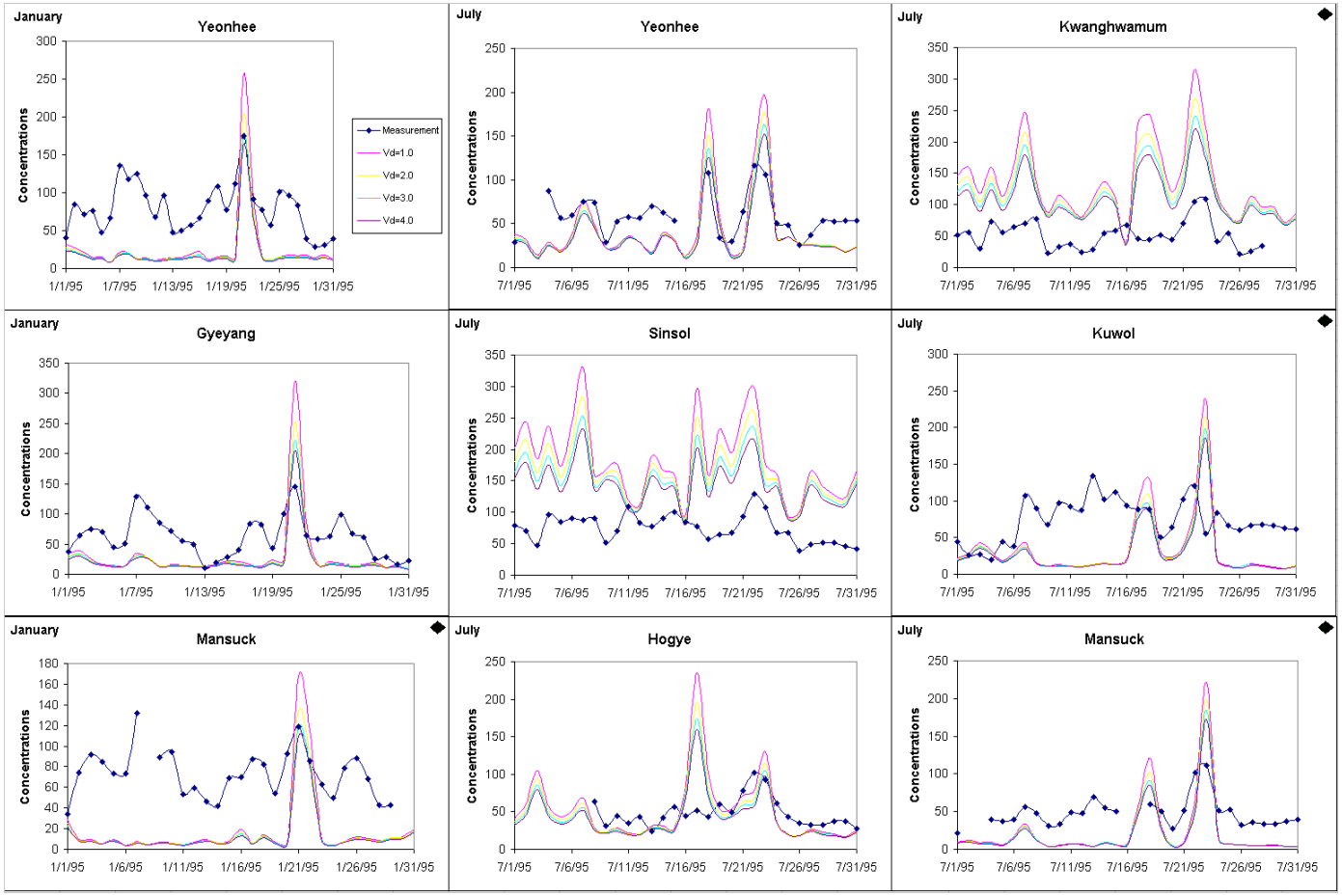

Figure #A3: Sensitivity of model predictions to dry deposition velocity over land and precipitation scavenging coefficient – Comparison to measured annual average concentrations, μg PM_{10}/m^3

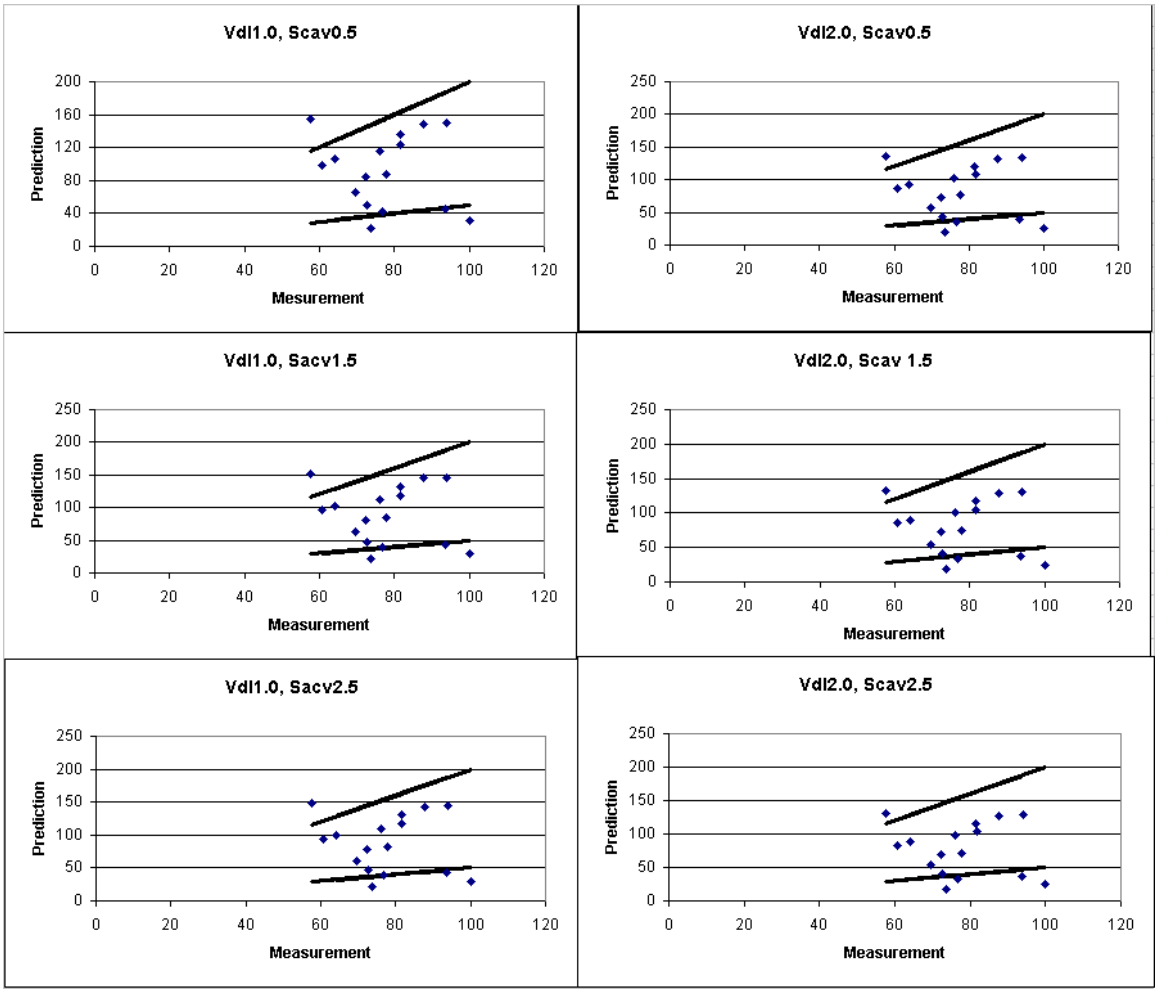

Figure #A3 Contd..

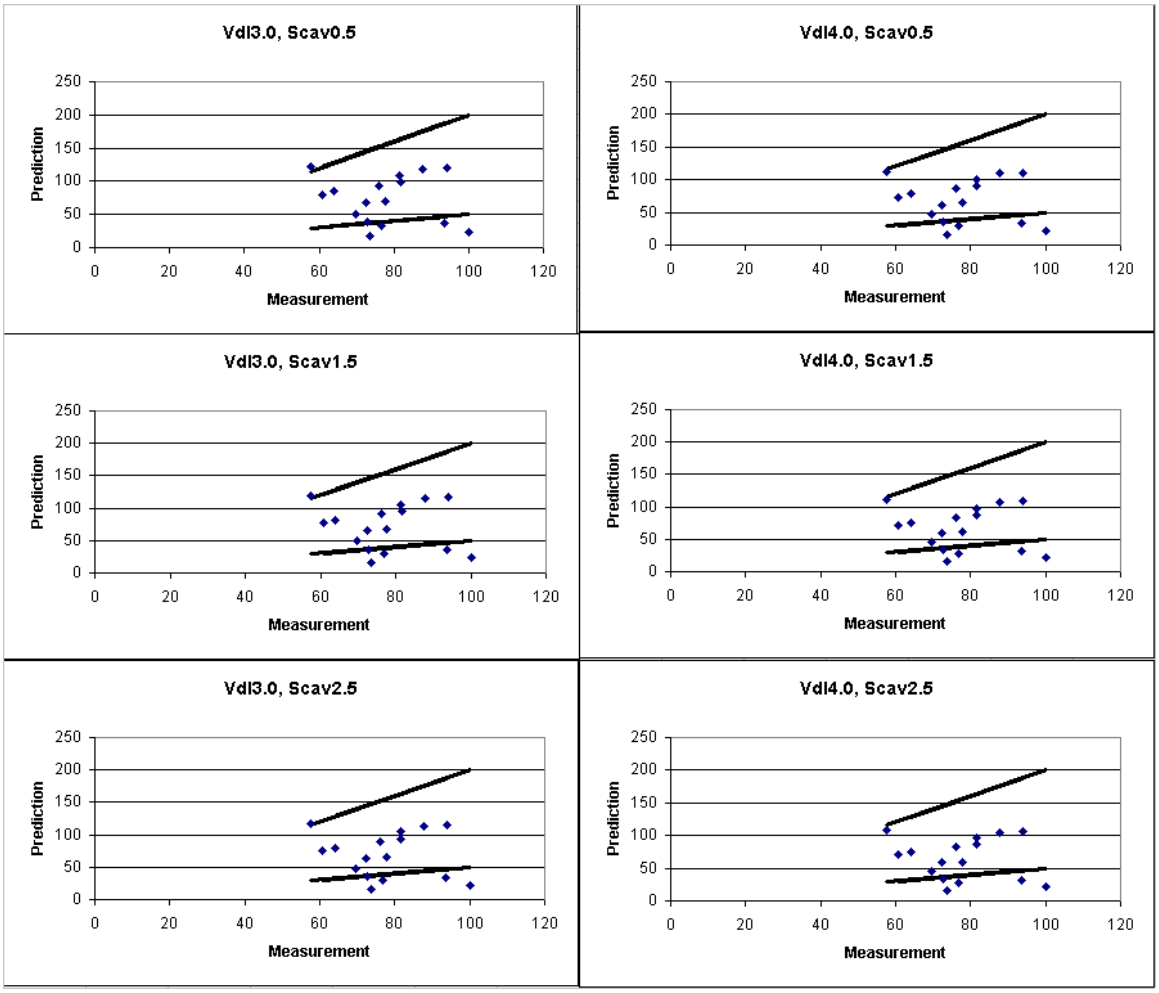

Figure #A4: Sensitivity of the model predictions to the variation of dry deposition velocity with Season /LS mask – Comparison to measured annual average concentrations, μg PM_{10}/m^3

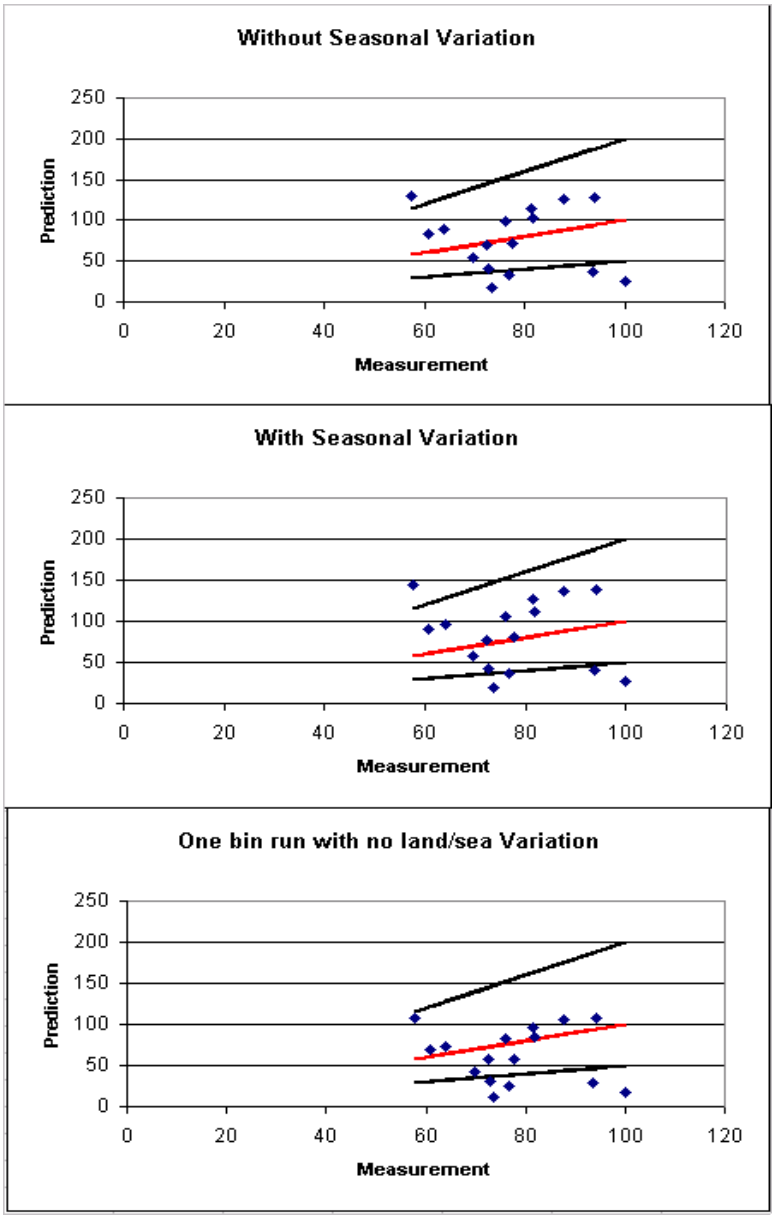

Figure #A5: Sensitivity of the model predictions to the variation of the meteorological conditions – Comparison to measured daily average concentrations, μg PM_{10}/m^3, for wind speeds uniformly capped and scaled at 4.0 m/sec

(a) January **(b) July**

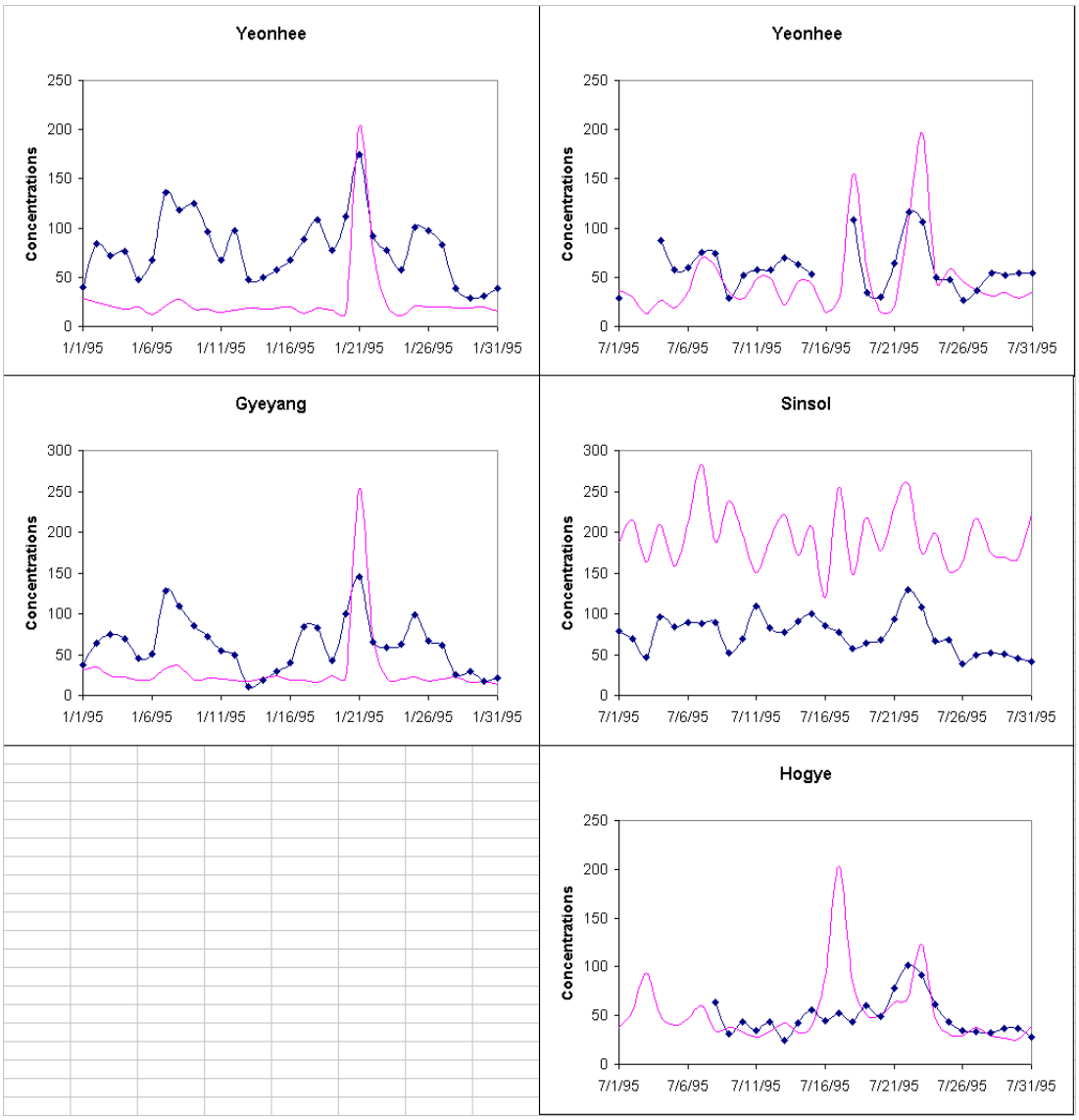

Figure #A6: Sensitivity of the model predictions to the emission inventory – Comparison to measured annual average concentrations, μg PM_{10}/m^3, for 50% cut down in fugitive dust coming from unpaved Roads

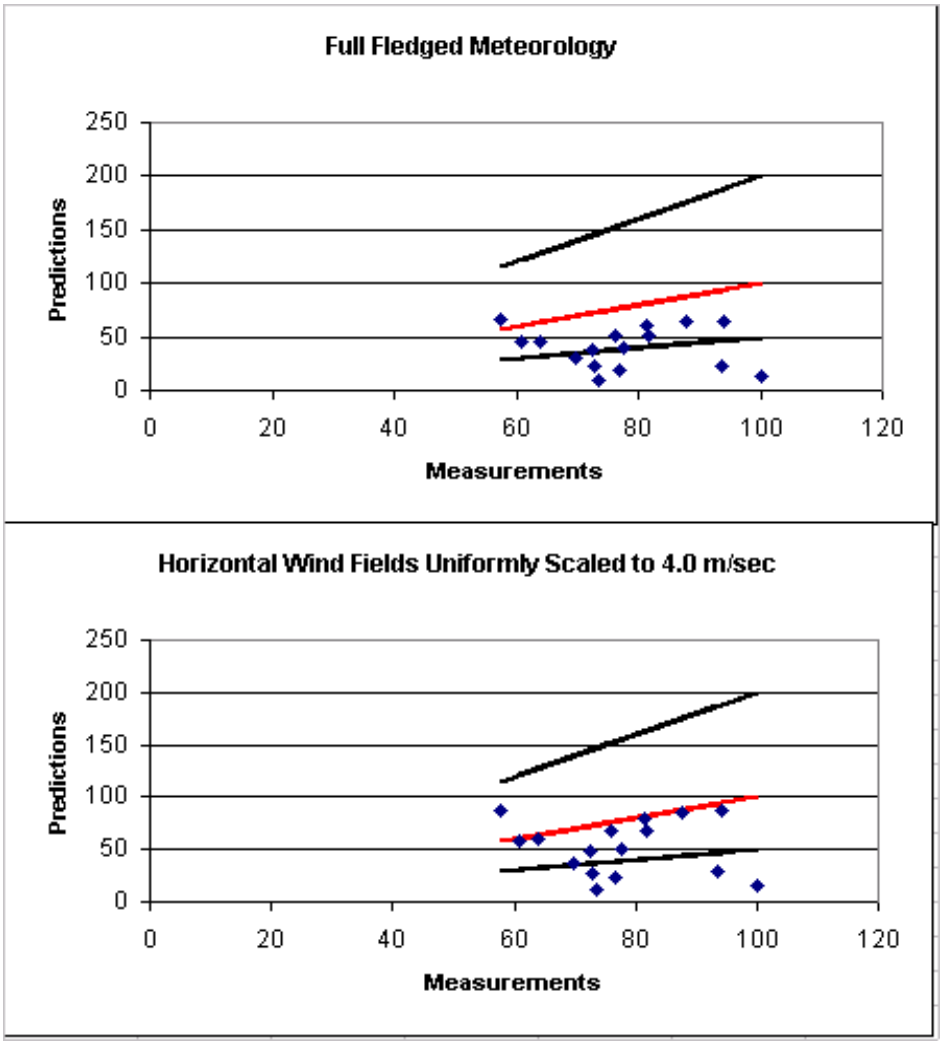

Figure #A7: Comparison of time series of model predicted daily average concentrations to measurements, μg PM_{10}/m^3 – Under normal meteorological conditions

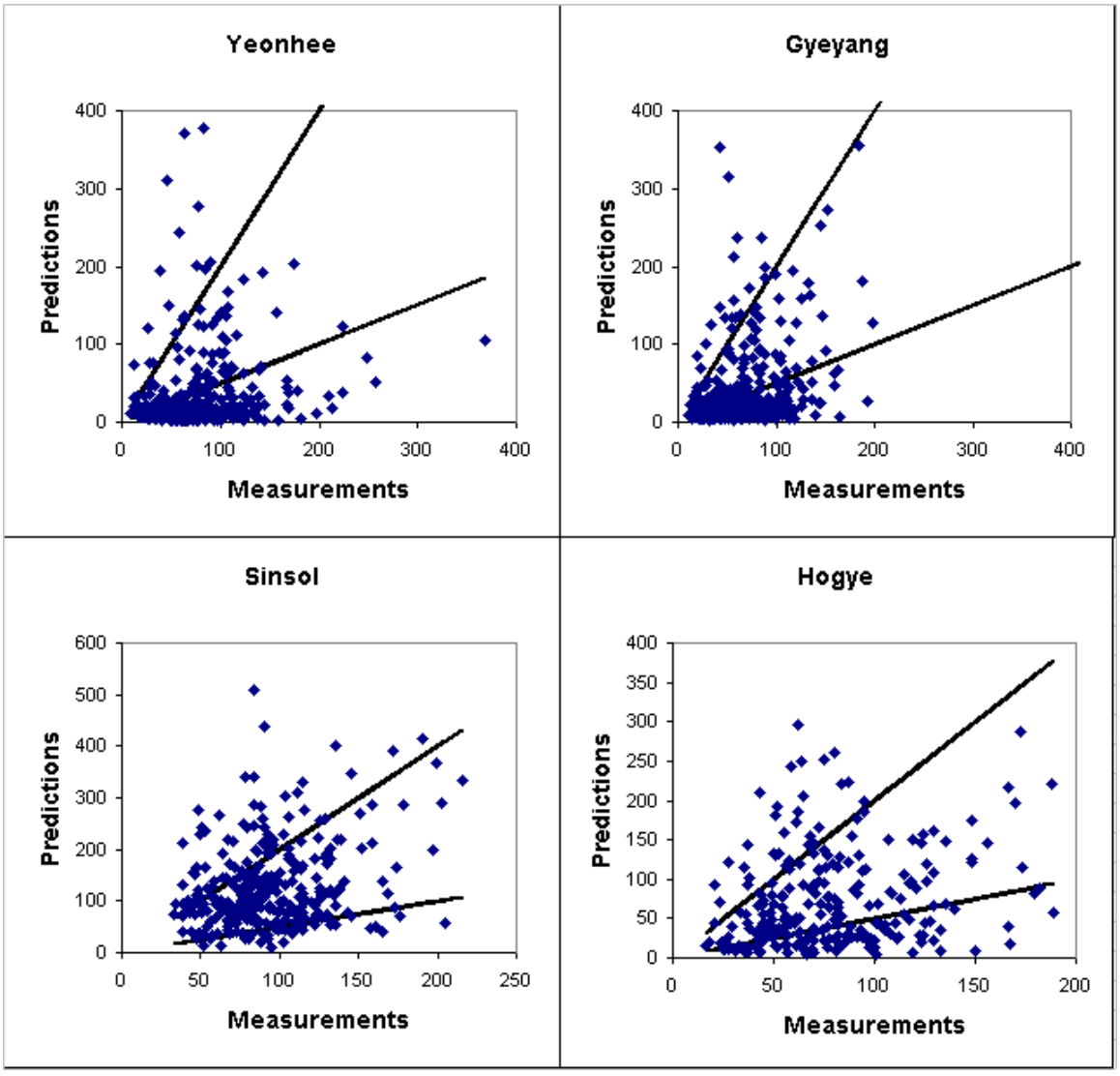

Figure #A8: Comparison of time series of model predicted daily average concentrations to measurements, μg PM_{10}/m^3 – Under horizontal wind speeds uniformly capped and scaled at 4.0 m/sec

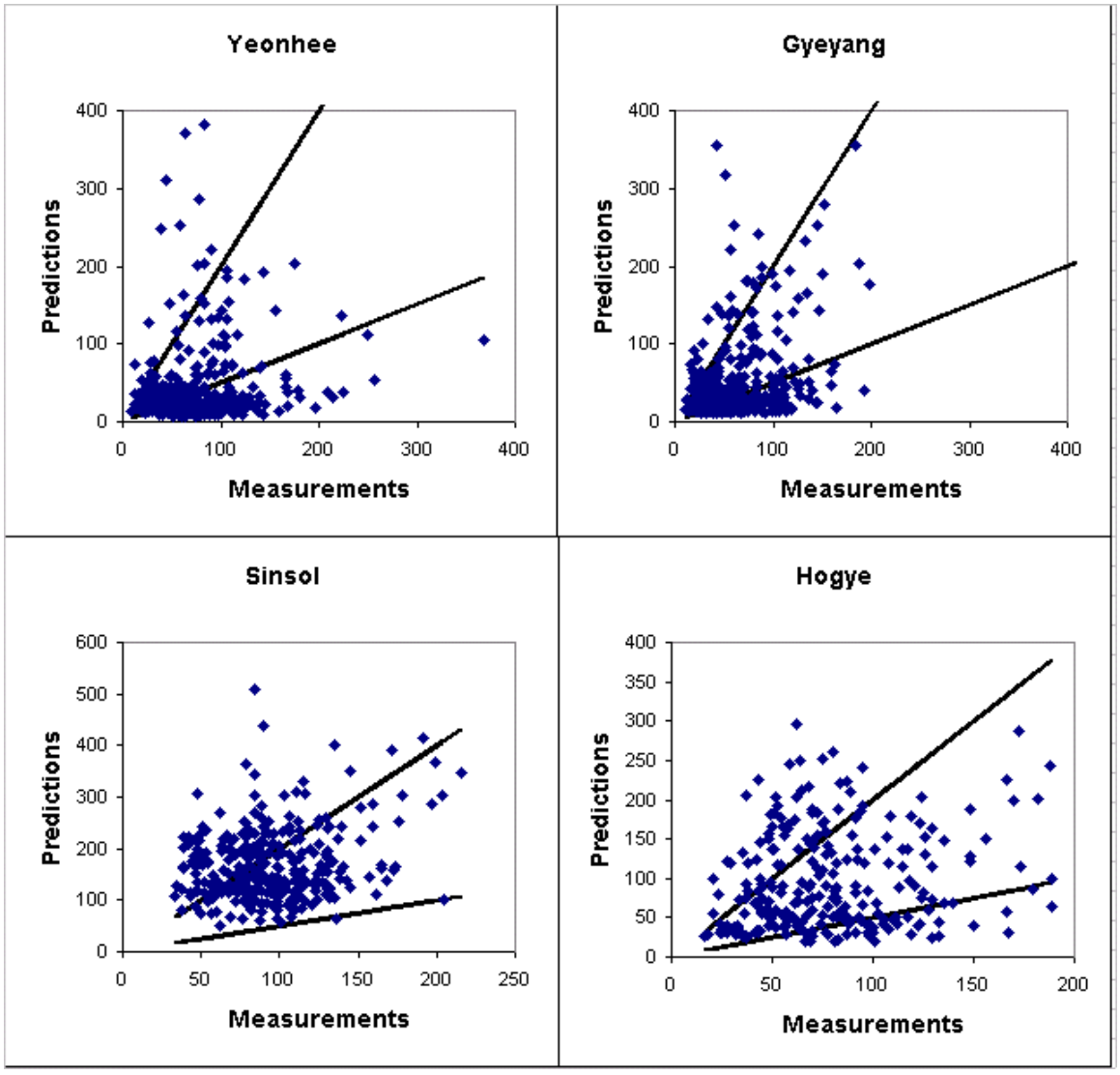

Figure #A9: Comparison of time series of model predicted daily average concentrations to measurements, μg PM_{10}/m^3 – Under normal meteorological conditions and with 50% Cut Down in emissions from unpaved road section.